TRANSLATIONALLY CONTROLLED TUMOUR PROTEIN AS A NOVEL THERAPEUTIC TARGET IN PULMONARY ARTERIAL HYPERTENSION

William Swinburne Foster

This thesis is submitted as a partial fulfillment of the Masters of Science program in

Cellular and Molecular Medicine

Faculty of Medicine

Department of Cellular and Molecular Medicine

University of Ottawa

ABSTRACT

Background: Pulmonary arterial hypertension (PAH) is a multifaceted disease characterized by elevated pulmonary arterial pressure, right ventricular hypertrophy, and a poor prognosis. Pathological hallmarks of PAH include pulmonary vascular remodelling, pre-capillary arterial obliteration, and plexiform lesions. Over the past 15 years, pulmonary endothelial cell (EC) apoptosis has been repeatedly implicated as a key trigger of occlusive arterial remodelling in PAH. While it has been hypothesized that pulmonary EC apoptosis gives rise to the emergence of growth-dysregulated, apoptosis-resistant ECs involved in arterial remodelling, the molecular mechanisms linking these two events has not yet been fully elucidated. Recently, our lab identified translationally controlled tumour protein (TCTP) as one of several significantly dysregulated proteins in culture-derived blood-outgrowth endothelial cells (BOECs) isolated from hereditable PAH (HPAH) patients harbouring mutations in the gene encoding for bone morphogenetic protein receptor type 2. Immunohistological analyses indicated that TCTP expression was associated with intra-luminal pulmonary ECs and inflammatory cells in the remodelled vessels of both human PAH patients and SU5416 rats. Furthermore, TCTP silencing abrogated excessive HPAH BOEC proliferation and promoted apoptosis *in vitro*.

Hypothesis: We hypothesized that TCTP represents a central molecular mechanism linking pulmonary arterial EC damage and apoptosis to the emergence of growth-dysregulated lung vascular cells and complex arterial remodelling in PAH.

Purpose: The purpose of the present thesis was to examine the effects TCTP inhibition on EC survival and TCTP abundance *in vitro* as well as on pulmonary hemodynamic changes and arterial remodelling *in vivo* using a well-validated rat model of severe PAH.

Methods: Inhibition of TCTP was accomplished using two TCTP small molecule inhibitors, sertraline and thioridazine. *In vitro*, rat lung microvascular ECs (RLMVECs) were exposed to thioridazine and assayed for TCTP abundance, survival, and markers of apoptosis. *In vivo*, PAH was induced in male Sprague Dawley rats using SU5416 combined with 3 weeks of chronic hypoxia (SU/CH). After 4 weeks, right ventricle systolic pressure (RVSP) was measured by direct catheterization and osmotic pumps containing either thioridazine or sertraline were implanted subcutaneously. Following 3 weeks of small molecule delivery, RVSP was re-evaluated, cardiac function/structure was determined using transthoracic echocardiography, and histological analyses of vascular remodelling and inflammation were performed.

Results: Our *in vitro* experiments demonstrated that thioridazine was able to significantly down-regulate TCTP levels and induce an apoptotic phenotype in RLMVECs. In the SU/CH rat model of severe PAH, both thioridazine and sertraline failed to have any effect on pulmonary hemodynamics, right ventricle structure/function, or vascular remodelling. Moreover, neither small molecule was able to detectably down-regulate TCTP levels in the lungs of SU/CH rats. Immunofluorescence staining revealed that TCTP expression occasionally corresponded with the expression of macrophage/monocyte marker CD68 in the lungs of SU/CH rats, consistent with its

expression by inflammatory cells; however, no significant differences were found in adventitial cell clearance in the presence or absence of the inhibitors.

Conclusions: Our findings support previous reports that thioridazine is able to significantly down-regulate TCTP and induce apoptosis *in vitro*. In contrast, both small molecule inhibitors failed to down-regulate lung TCTP levels or have any beneficial effects on the progression of PAH in SU/CH rats.

TABLE OF CONTENTS

LIST OF TABLES

LIST OF FIGURES

LIST OF ABBREVIATIONS

7AAD	7-aminoactinomycin D
α-SMA	Alpha smooth muscle actin
ALK-1	Activin-like kinase type-1
ANOVA	Analysis of variance
APAH	Associated pulmonary arterial hypertension
BMP	Bone morphogenetic protein
BMPR2	Bone morphogenetic protein receptor type 2
BOEC	Blood outgrowth endothelial cell
CAV-1	Caveolin1
CO	Cardiac output
CCB	Calcium channel blocker
cGMP	Cyclic guanosine mono-phosphate
CH	Chronic hypoxia
CMC	Carboxymethyl cellulose
DMSO	Dimethyl sulfoxide
EC	Endothelial cell
ENG	Endoglin
eNOS	Endothelial nitric oxide synthase
ERA	Endothelin receptor antagonist
ET-1	Endothelin-1
H+E	Hematoxylin + eosin
HIF-1α	Hypoxia inducible factor 1 alpha
HIV	Human immunodeficiency virus
HPAH	Hereditary pulmonary arterial hypertension
HR	Heart rate
HRF	Histamine releasing factor
IPAH	Idiopathic pulmonary arterial hypertension
LVID,d	Left ventricular internal diameter at diastole
MCT	Monocrotaline
MDM2	Murine double minute 2
NO	Nitric oxide
NOS	Nitric oxide synthase
PA	Pulmonary artery
PAAT	Pulmonary arterial acceleration time
PAH	Pulmonary arterial hypertension
PAP	Pulmonary arterial pressure
PBS	Phosphate buffered saline
PCNA	Proliferating cell nuclear antigen
PDE-5	Phosphodiesterase-5
PDE-5i	Phosphodiesterase-5 inhibitiors
PEG	Polyethylene glycol
PET	Pulmonary ejection time
PGI_2	Prostacyclin
PH	Pulmonary hypertension

PVR	Peripheral vascular resistance
R-Smad	Receptor-mediated Smad
RIPA	Radioimmunoprecipitation assay
RLMVEC	Rat lung microvascular endothelial cell
RNA	Ribonucleic acid
ROS	Reactive oxygen species
RVfWT	Right ventricle free wall thickness
RVH	Right ventricle hypertrophy
RVID,d	Right ventricular internal diameter at diastole
RVSP	Right ventricular systolic volume
SAP	Systemic arterial pressure
SDS-PAGE	Sodium dodecyl sulfate - polyacrylamide gel electrophoresis
SEM	Standard error of the mean
SERT	Serotonin transporter
sGC	Soluble guanylate cycliase
shRNA	Short hairpin RNA
SMAD9	Mothers against decapentaplegic 9
SSRI	Selective serotonin uptake inhibitor
STS	Staurosporine
SU	SU5416
SU/CH	SU5416/chronic hypoxia
SV	Stroke volume
TAPSE	Tricuspid annular plane systolic excursion
TCTP	Translationally controlled tumour protein
TGF	Transforming growth factor
TGF-β	Transforming growth factor beta
TUNEL	Terminal deoxynucleotidyl transferase dUTP nick end labeling
VEGF	Vascular endothelial growth factor
VEGFR2	Vascular endothelial growth factor receptor 2
VTI	Velocity time integral

ACKNOWLEDGEMENTS

The work contained within this thesis would not have been possible without the on-going support of my family, friends, and colleagues. First and foremost, I would like to thank my supervisor Dr. Duncan J. Stewart for his mentorship and guidance throughout my graduate studies. I would also like to thank Dr. David Courtman and Dr. Shirley Mei for their assistance with experimental planning and for providing their invaluable technical insights.

For the *in vivo* experiments presented in this thesis, I would like to acknowledge the incredible help of Dr. Yupu Deng. Dr. Deng's technical expertise allowed me to design robust experiments with a variety of critical physiological measurements. I would also like to sincerely thank Mohamad Taha, Colin Suen, and Dr. Ketul Chadharry for helping me navigate the intricacies of the SU/CH rat model and for their willingness to discuss experimental designs over coffee.

To all of my colleagues in Dr. Stewart's lab, I would like to thank you for your friendship and support. You all made my time at the Stewart lab truly enjoyable. Finally, I would like to thank the Canadian Institutes of Health Research and the University of Ottawa for generously supporting my graduate research.

LIST OF ORIGINAL PUBLICATIONS

As a Masters of Science candidate I have had the privilege of collaborating with colleagues from the University of Ottawa, the Ottawa Hospital Research Institute, and University of Cambridge on several original research projects and research-related journal articles. These publications are presented below in chronological order:

Lavoie, J. R., Ormiston, M. L., Perez-Iratxeta, C., Courtman, D. W., Jiang, B., Ferrer, E., Caruso, P., Southwood, M., Foster, W. S., Morrell., N.W., & Stewart, D. J. (2014). Proteomic analysis implicates translationally controlled tumor protein as a novel mediator of occlusive vascular remodeling in pulmonary arterial hypertension. *Circulation, 129*(21), 2125-2135.

Foster, W. S.,* Putos, S. M.* (2014). Neglecting the null: the pitfalls of underreporting negative results in preclinical research. *University of Ottawa Journal of Medicine, 4*(1), 31-33. *Co-first authors.

Foster, W.S., Suen, C.M., & Stewart, D.J. (2014) Regenerative cell and tissue-based therapies for the treatment of pulmonary arterial hypertension. *Can J Cardiol. 30*(11)*,* 1150-1160.

INTRODUCTION

1.1 Pulmonary Arterial Hypertension (PAH)

1.1.1 Clinical Classification & Epidemiology

According to expert consensus, pulmonary hypertension (PH) is a pathophysiological state in which mean pulmonary arterial pressure (PAP) is ≥ 25 mmHg in the setting of normal or reduced cardiac output (CO) (Archer et al., 2010). Over the past four decades the clinical classification of PH has undergone several iterations as our understanding of the disease has developed and the need to classify distinct forms of the disease has emerged. At the World Health Organization Conference on PH in 1973, two basic categories of PH were first created: 1) primary PH; and 2) secondary PH according to the presence of identified causes or risk factors (Hatano et al., 1975). These categories remained unchanged until the second World Symposium on PH in Evian, France in 1998, during which the modern five group classification system was implemented (Simonneau et al., 2004). Since this meeting, the original five group system has been regularly updated at subsequent PH symposia. According to the most recent clinical guidelines, established at the 2013 World Symposium in Nice, France, the 5 clinical classifications of PH are as follows: Group 1, pulmonary arterial hypertension (PAH); Group 1', pulmonary veno-occlusive disease and/or pulmonary capillary hemangiomastosis; Group 1", persistent PH of the newborn; Group 2, PH due to left heart disease; Group 3, PH due to lung diseases and/or hypoxia; Group 4, chronic thromboembolic PH; and Group 5, PH with unclear multifactorial mechanisms (Simonneau et al., 2013) (Table 1).

Group 1 PH, or PAH, is defined as PH in the absence of left heart disease (i.e. pulmonary arterial wedge pressure of ≤ 15 mmHg), parenchymal lung disease, or other

causes of PH (i.e. pulmonary emboli) (Simonneau et al., 2013). Unlike other forms of PH, PAH primarily affects the pulmonary arteries and pre-capillary arteriole bed (Barst et al., 2004; McLaughlin & McGoon, 2006). PAH can be subdivided into four subgroups based on pathophysiological mechanisms and/or associated conditions: 1.1, idiopathic or sporadic PAH (IPAH); 1.2, heritable PAH (HPAH); 1.3, drug and/or toxin induced PAH; and 1.4, PAH associated (APAH) with connective tissue disease, human immunodeficiency virus (HIV) infection, portal hypertension, congenital heart disease, or schistosomiasis (Barst et al., 2004) (Table 1). The content of this thesis focuses primarily on HPAH and IPAH, but the underlying mechanisms explored are likely relevant to all forms of PAH since they share similar pathological features, as described below.

Epidemiological data from the Registry to Evaluate Early and Long-term Pulmonary Arterial Hypertension Disease Management (REVEAL Registry) reports a 5-year survival rate of 57% for patients with IPAH/HPAH in the United States (period 2006-2009) (Benza et al., 2012). Thus, despite advancements in disease management and an increased number of available PAH therapies, the prognosis for patients with PAH remains poor.

Table 1. Updated clinical classification of pulmonary hypertension.

1. Pulmonary arterial hypertension (PAH)
    - 1.1 Idiopathic PAH (IPAH)
    - 1.2 Heritable PAH (HPAH)
        - 1.2.1 BMPR2
        - 1.2.2. ALK-1, ENG, SMAD9, CAV1, KCNK3
        - 1.2.3. Unknown
    - 1.3. Drug and toxin induced
    - 1.4. Associated with:
        - 1.4.1 Connective tissue disease
        - 1.4.2 HIV infection
        - 1.4.3 Portal hypertension
        - 1.4.4 Congenital heart diseases
        - 1.4.5 Schistosomiasis

1'. Pulmonary veno-occlusive disease and/or pulmonary capillary hemangiomastosis

1". Persistent pulmonary hypertension of the newborn

2. Pulmonary hypertension due to left heart disease
    - 2.1 Left ventricular systolic dysfunction
    - 2.2 Left ventricular diastolic dysfunction
    - 2.3 Valvular disease
    - 2.4 Congenital/acquired left heart inflow/outflow tract obstruction and congenital cardiomyopathies

3. Pulmonary hypertension due to lung disease and/or hypoxia
    - 3.1 Chronic obstructive pulmonary disease
    - 3.2 Interstitial lung disease
    - 3.3 Other pulmonary diseases with mixed restrictive and obstructive pattern
    - 3.4 Sleep-disordered breathing
    - 3.5 Alveolar hypoventilation disorders
    - 3.6 Chronic exposure to high altitude
    - 3.7 Developmental lung diseases

4. Chronic thromboembolic pulmonary hypertension (CTEPH)

5. Pulmonary hypertension with unclear multifactorial mechanisms
    - 5.1 Hematologic disorders: chronic hemolytic anemia, myeloproliferative disorders, splenectomy
    - 5.2 Systemic disorders: sarcoidosis, pulmonary histiocytosis, lymphagiomyomatosis
    - 5.3 Metabloic disorders: glycogen storage disease, Gaucher disease, thyroid disorders
    - 5.4 Others: tumoral obstruction, fibrosing mediastinitis, chronic renal failure, segmental PH

Adapted from Simonneau G et al., 2013.

1.1.2 PAH Pathophysiology

1.1.2.1 Overview

In healthy adults the pulmonary circulation is a low pressure, low impedance system that serves the vital function of gas exchange. The pulmonary arteries are responsible for transporting de-oxygenated blood from the right ventricle to the lungs for re-oxygenation. Following the exchange of CO_2 for O_2 at the level of the alveoli, the pulmonary veins transport re-oxygenated blood back to the left side of the heart where it is subsequently distributed throughout the body via the systemic circulation. Unlike any other arterial bed of the body, the pulmonary circulation is arranged in series with the systemic circulation and must therefore accommodate the entire CO. The normal lung is remarkable in that it can accept the entire CO with arterial pressures that are little more than those of the venous bed. In healthy individuals, this occurs even during large increases in CO, such as those experienced during exercise. In patients with PAH, this ability is lost due to a reduction in the available cross-sectional area of the lung arteriolar bed (Archer et al., 2010). This can occur by a variety of mechanisms, which may be more or less important in any given patient. For example, in a small subset of PAH patients, an increase in pulmonary vascular resistance (PVR) occurs due to sustained vasoconstriction (Sitbon et al., 2005). These patients can be identified by acute vasodilator responsiveness testing at the time of diagnostic cardiac catheterization and are essentially cured by the use of calcium channel blockers (CCBs) (Sitbon et al., 2005). In contrast, vasoconstriction is thought to play only a minor role, if any, in the vast majority of PAH patients, and CCBs are in fact contraindicated in patients that do not show vasodilator responsiveness (Sitbon et al., 2005). Thus, the loss of effective lung arteriolar

microcirculation in most PAH patients occurs due to the progressive remodelling of the pulmonary arteries and arterioles, resulting in vascular narrowing and even obliteration (Archer et al., 2010). Together these pathological processes lead to increases in PVR and PAP thereby exposing the right ventricle to chronic pressure overload (Ryan & Archer, 2014). After a period of adaptive myocardial hypertrophy, the right ventricle transitions from a compensated to decompensated state, characterized by maladaptive remodelling, progressive chamber dilatation, and contractile weakening (Voelkel et al., 2006). Ultimately, these progressive changes contribute to right ventricle failure and the inability to maintain CO, the main cause of mortality for patients with PAH (Campo et al., 2011; D'Alonzo et al., 1991).

1.1.2.2 Endothelial Dysfunction & Vasoactive Imbalances

The pulmonary endothelium constitutes the innermost layer of the pulmonary arteries and plays a major role in the regulation of vascular structure and function via the release of potent endothelial-derived vasoactive factors, such as endothelin-1 (ET-1), prostacyclin (PGI_2), and nitric oxide (NO) (Christman et al., 1992; Giaid & Saleh, 1995; Giaid et al., 1993; Tuder et al., 1999). It is widely accepted that endothelial dysfunction plays a key role in the progression of PAH (Budhiraja et al., 2004; Jurasz et al., 2010; Sakao et al., 2009). In PAH patients, endothelial dysfunction is evidenced by an increased release of vasoconstrictors (i.e. ET-1 and thromboxane A2) and a reduction in the release of vasodilators (i.e. PGI_2 and NO) leading to chronic vasoconstriction (Humbert et al., 2014). Concomitantly, decreased expression of endothelial nitric oxide synthase (eNOS), the enzyme which catalyzes the production of NO from L-arginine, have also been

reported in PAH patients (Giaid & Saleh, 1995), however this finding has not been reproduced by others (Mason et al., 1998). To date, nearly all pharmacotherapies for PAH have focused on restoring vasoactive imbalances associated with endothelial dysfunction. These therapies have primarily targeted the PGI_2, ET-1, or NO pathways (Perrin et al., 2015).

1.1.3 Current Therapies for PAH

1.1.3.1 Prostacyclin Analogues

A member of the eicosanoid family, PGI_2 is an endogenous lipid molecule produced predominantly by endothelial cells (ECs) through the conversion of arachidonic acid by the enzyme prostacyclin synthase. PGI_2 acts as a potent vasodilator of the vascular bed by binding to prostacyclin receptors and inducing smooth muscle relaxation. Additionally, PGI_2 has been shown to be anti-proliferative and can inhibit platelet aggregation (Jones et al., 1995). Due to the short half-life and poor stability of PGI_2 in solution, multiple PGI_2 analogues have been synthesized and utilized for the treatment of PAH (Perrin et al., 2015). In North America, clinically approved PGI_2 analogues include epoprostenol and treprostinil; however, additional PGI_2 analogues, such as iloprost and beraprost, have been approved for PAH in other countries. More recently, the highly selective and potent prostacyclin receptor agonist selexipag has emerged as novel PGI_2 analogue for PAH (Pullamsetti et al., 2014). In December 2015, a phase III multicenter, double-blind, placebo-controlled clinical trial performed in 1156 patients with PAH trial found that selexipag significantly reduced the the risk of morbidity/mortality event versus placebo control (Sitbon et al., 2015).

1.1.3.2 Endothelial Receptor Antagonists

Elevated levels of ET-1 were first identified in the lungs of primary PH patients in the early 1990s (Giaid et al., 1993; Stewart et al., 1991). Since this seminal discovery, the translation and widespread adoption of endothelin receptor antagonists (ERAs) for the treatment of PAH has become common practice. ET-1 is an endogenous vasoconstrictor that regulates pulmonary smooth muscle tone by binding to ET_A or ET_B receptors (Kim & Rubin, 2002). ET_A and ET_B receptors can be found on the outer membrane of pulmonary artery smooth muscle cells where they mediate vasoconstriction via the regulation of intracellular calcium levels (Clozel et al., 1992; Neylon et al., 1994). However, ET_B receptors can also be found on the outer membrane of pulmonary ECs where they facilitate the release of the vasodilators PGI_2 and NO (Masaki et al., 1999). There are currently three ERAs approved for the treatment of PAH: 1) bosentan, a competitive specific dual $ET_{A/B}$ receptor antagonist; 2) ambrisentan, a highly selective ET_A receptor antagonist (Perrin et al., 2015); and 3) macitentan, a tissue-targeting dual ERA with comparatively slower receptor dissociation kinetics than both bosentan and ambrisentan (Gatfield et al., 2012).

1.1.3.3 Modulators of the Nitric Oxide Pathway

In the pulmonary vasculature, NO is produced by pulmonary ECs following the conversion of L-arginine to L-citrulline by NO synthase (NOS). Evidence of reduced NOS expression in PAH highlights the importance of this pathway in regulating vascular homeostasis and relevancy as a therapeutic target (Giaid & Saleh, 1995). NO is a potent endogenous vasodilator that regulates pulmonary vessel tone by stimulating soluble

guanylate cyclase (cGC). When stimulated, cGC catalyses the synthesis of the second messenger cyclic guanosine mono-phosphate (cGMP). cGMP subsequently induces smooth muscle relaxation (Archer et al., 2010). Phosphodiesterase-5 (PDE-5) is an endothelial-specific PDE isoform that degrades cGMP and, thus, inhibits smooth muscle vasoconstriction. PDE-5 inhibitors (PDE-5i) induce smooth muscle vasoconstriction by inhibiting PDE-5 activity thereby preventing the degradation of cGMP. Currently, sildenafil and tadalafil are the only clinically approved PDE-5i for the treatment of PAH (Perrin et al., 2015).

In addition to PDE-5i, soluble guanylate cyclase (sGC) stimulators have also been shown to modulate the activity of the NO pathway. In PAH, the ability of NO to bind cGC is is attenuated due to reduced NO bioavailability and conformational changes in the enzyme receptor (Stasch et al., 2011). cGC stimulators restore NO signalling by stimulating the activity of cGC and promoting cGN-NO binding (Stasch et al., 2011). Thus, much like PDE-5i, cGC stimulators promote smooth muscle cell relaxation by increasing the concentration of cGMP. Riociguat recently became the first cGC stimulator therapy approved for the treatment of PAH (Makowski et al., 2015).

1.1.4 Newer Concepts in the Pathogenesis of PAH

The pathogenesis of PAH has been the focus of intensive clinical and pre-clinical research for many decades. Unfortunately, due to the limited availability of early-disease patient materials, identifying the specific mechanisms that contribute to the initiation and development of PAH has proven to be a considerable challenge. At present the focus

remains on identifying the predisposing conditions and aggravating stimuli that give rise to increased PVR.

While the concept of endothelial dysfunction has led to a number of effective and specific therapies for PAH, it has become increasingly clear that the pathophysiology of this disease is far more complex than originally thought. The current overarching theory in the literature is often referred to as the "multi-hit" or "two-hit" hypothesis (McLaughlin & McGoon, 2006). According to this hypothesis, the pulmonary endothelium becomes permanently damaged following the interaction of a predisposing state (i.e. genetic susceptibility or pre-existing disease) with one or more environmental stimuli (McLaughlin & McGoon, 2006). Such stimuli may include anorexigens, elevated levels of serotonin, HIV, reactive oxygen species (ROS), inflammatory cytokines (i.e. IL-6), or chronic sheer stress due to congenital heart disease (Figure 1) (Budhiraja et al., 2004). However, at present it is likely that the "second hit" is an unidentified stimulus or stress and may involve additional unknown genetic modifiers.

1.1.4.1 Genetic Susceptibility in PAH: Bmpr2 Mutations

Genetic studies of individuals with PAH have led to the identification of several PAH disease-causing genes which may predispose individuals to endothelial damage and subsequent pathological processes (Simonneau et al., 2004; Simonneau et al., 2013). Recent data indicates that approximately 75% of individuals with HPAH, and up to 25% of patients with IPAH without any family history of the disease, harbour heterozygous mutations in the gene encoding for bone morphogenetic protein receptor 2 (BMPR2) (Machado et al., 2009). BMPR2 is a member of the transforming growth factor (TGF)-β

super-family of transmembrane serine/threonine kinase receptors and is involved in paracrine signalling (Machado et al., 2009). The importance of BMPR2-mediated signalling in the regulation of EC processes such as growth, differentiation, and apoptosis has been well documented by our group and others (Miyazono et al., 2005; Teichert-Kuliszewska et al., 2006). Although BMPR2 is ubiquitous, it is abundant in pulmonary artery ECs and minimally expressed in pulmonary artery smooth muscle cells and fibroblasts, thus suggesting a key role in EC biology (Atkinson et al., 2002; Machado et al., 2009). All together there are seven known bone morphogenetic protein (BMP) type receptors, which are classified as either type 1 or type 2. BMPR2 receptors are located at the cell membrane and initiate intracellular signalling cascades in response to BMP-2, -4, -6, -7, and -9, and the growth differentiation factors 5 and 6 (Atkinson et al., 2002; Teichert-Kuliszewska et al., 2006). When a BMP ligand is present, BMPR2 forms a heterodimer with an available type 1 receptor. Once bound in a heterodimeric complex, BMPR2 phosphorylates the type 1 receptor initiating an intracellular signalling cascade involving the receptor-mediated Smads (R-Smads), namely Smads 1/5/8. Signal transduction by R-Smads culminates in the formation of R-Smad/Co-Smad complexes, which subsequently translocate into the nucleus and regulate gene expression (Schmierer & Hill, 2007). *In vitro* studies have demonstrated that that loss of BMPR2 signalling increases the susceptibility of pulmonary artery ECs to apoptosis and increases proliferation in smooth muscle cells (Atkinson et al., 2002). Thus, our group has proposed that *Bmpr2* mutations may increase the susceptibility of pulmonary ECs to apoptosis in the event of vascular damage and promote smooth muscle cell hyperplasia (Teichert-Kuliszewska et al., 2006).

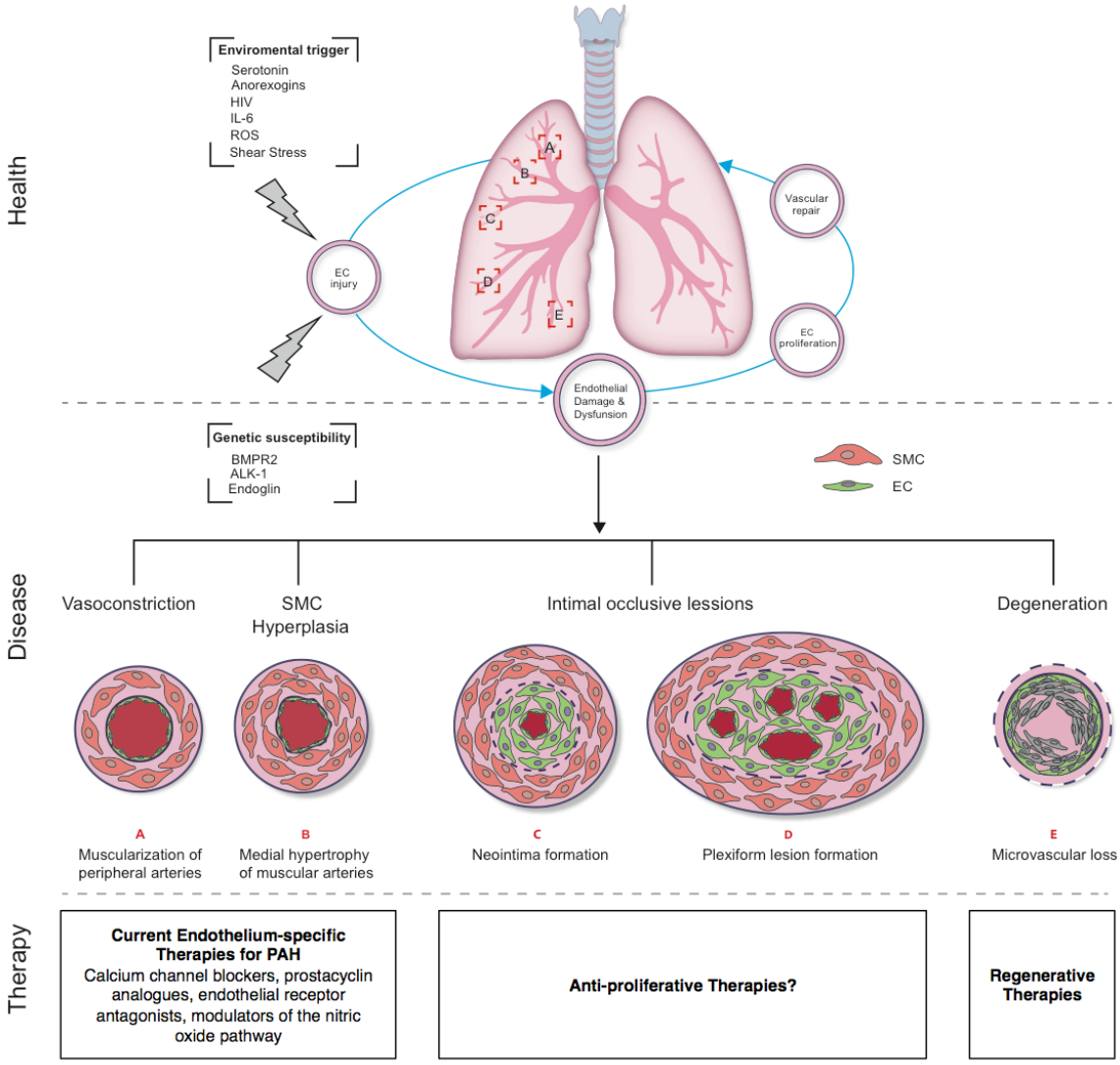

Figure 1. Pathophysiological overview and modern therapeutic strategies for the treatment of PAH. Exposure to environmental insults such as increased serotonin levels, anorexigens, viruses, inflammatory cytokines such as interleukin 6 (IL-6), or sheer stress can contribute to endothelial cell (EC) damage and injury. In healthy individuals, physiological repair processes restore normal lung function via the proliferation of nearby ECs and/or the recruitment of circulating endothelial progenitor cells (EPCs). Alternatively, in PAH, pulmonary vascular cell damage contributes to the degeneration of microvasculature and/or proliferative arteriolar remodelling. In patients with hereditary PAH, underlying genetic mutations to the genes encoding for bone morphogenetic protein receptor type 2 (*Bmpr2*), activin-like receptor kinase-1 (ALK-1), and endoglin are associated with an increased susceptibility to EC damage and injury. Traditional pharmacotherapies aimed at restoring imbalances in vasoactive factors are presented alongside hypothetical anti-proliferative therapies and regenerative therapies. Adapted from Foster et al., 2014.

Other rare genetic mutations in genes involved in TGF-β signalling have also been identified in 5% of HPAH patients (Simonneau et al., 2013). These mutations affect the genes encoding for activin-like kinase type-1 (ALK-1) (Harrison et al., 2003), endoglin (Chaouat et al., 2004), and mothers against decapentaplegic 9 (Smad9) (Nasim et al., 2011). Interestingly, unlike other TGF-β receptors, ALK-1 signalling occurs via Smads 1/5 rather than 2/3 (Morrell et al., 2006). As well, the recent discovery of mutations in SMAD9 associated with HPAH (Nasim et al., 2011) underscores the central role of abnormalities in BMP signalling in PAH pathogenesis. Coupled with the observation that BMPR2 expression is consistently reduced in IPAH patients, even in the absence of any detectable mutation in this pathway, these findings suggest that BMPR2-mediated signalling is critical for the maintenance of lung endothelial and vascular homeostasis. Nonetheless, additional PAH-associated mutations that are not directly involved in TGF-β signalling have also been identified in HPAH. These include caveolin1 (*CAV-1*) (Austin et al., 2012), a gene encoding the endothelial membrane protein caveolae, and *KCNK3*, a gene encoding the potassium channel super family K member-3 (Austin et al., 2012; Ma et al., 2013). While the specific mechanisms by which both *CAV-1* and *KCNK3* mutations are linked to HPAH remain unknown, the fact that they are not part of the TGF-β signalling pathway may point to interesting new avenues for PAH research.

1.1.4.2 Experimental Models of PAH

Experimental models are invaluable to understanding PAH pathobiology and facilitating translational research. For this thesis, experimental models will be referred to as "PH" models and the term "PAH" will be reserved for the human condition, with one

exception as discussed below. While numerous animal models of PH have been developed in several species, until recently, these models only partially reproduced the salient characteristics of human PAH. Typically, researchers have relied upon rat models most heavily due to the fact that the rat displays greater inherent susceptibility to developing PH in response to chronic hypoxia (CH), EC injury, or a combination of both (Maarman et al., 2013). The two rat models that are most commonly utilized to recreate PH *in vivo* are the monocrotaline model (i.e. the MCT model) and the "severe PAH" model induced by administration of a single dose of SU5416 (SU), a vascular endothelial growth factor receptor 2 (VEGFR2) inhibitor, in combination with exposure to CH (i.e. the SU/CH model) (Maarman et al., 2013). Although other rat models of PAH are also utilized, namely the CH alone model, such models may be more reliable for studying Group 3 PH caused by hypoxia or lung disease (Ryan et al., 2011). Therefore, I have limited the discussion in this section to include rat models that best reproduce the pathological conditions associated with Group 1 PH.

1.1.4.3 The MCT Rat Model

The ability of monocrotaline (MCT) to induce PAH in rats was initially reported in 1967 by Kay and colleagues after noticing that young rats fed a diet containing *crotalaria spectabilis* seeds spontaneously developed right ventricle hypertrophy (RVH), elevated right ventricular systolic pressure (RVSP), and medial thickening of the pulmonary arteries (Kay et al., 1967). It was later discovered that these seeds contained a plant alkaloid that upon being metabolized by liver enzyme cytochrome-P450 into pyrrolic derivatives (i.e. MCT) was capable of inflicting EC injury (Shah et al., 2005).

Since this report, the MCT model has been widely employed as a standard model of PAH due to its simplicity, feasibility, and reproducibility (Maarman et al., 2013). In accordance with modern conventions, the MCT model is initiated by a single subcutaneous or intraperitoneal injection of MCT in suspension (60-80 mg/kg) (Maarman et al., 2013). In addition to increases in RVH and RVSP, the pulmonary arteries of MCT rats display some histological features of human PAH including intimal hyperplasia, medial hypertrophy, adventitial thickening, and inflammation (Maarman et al., 2013) .

The widespread use of the MCT model has undoubtedly facilitated an improved understanding of PAH pathobiology and served as a platform for the development of modern-day PAH therapies. However, MCT rats lack key histological features of human PAH, such as evidence of complex arterial remodelling and plexiform lesions (Gomez-Arroyo et al., 2012). While some investigators have succeeded in creating plexiform-like lesions in the model by combining MCT with a unilateral pneumonectomy procedure to increase pulmonary arterial shear stress (Okada et al., 1997; White et al., 2007), such procedures add considerable technical difficulty to the model and can increase morbidity and mortality. This presents a substantial problem given that the long-term survival of MCT rats is typically poor, potentially due to the off-target effects of MCT (Stenmark et al., 2009). Another limitation is that rats exposed to MCT seem to respond to a variety of therapies that fail to yield beneficial results in human PAH patients (Maarman et al., 2013; Stenmark et al., 2009). This discrepancy highlights a potential pitfall of the MCT model for use in translational research.

1.1.4.4 The SU/CH Rat Model

PAH is induced in the SU/CH rat model by combining a single subcutaneous injection of SU5416 suspended in carboxymethyl cellulose (CMC) with three consecutive weeks of exposure to CH (~10% O_2) (Abe et al., 2010; Taraseviciene-Stewart et al., 2001). This SU/CH model was first reported in 2001 by Taraseviciene-Stewart and colleagues in conjunction with their work on vascular endothelial growth factor (VEGF) in PAH (Taraseviciene-Stewart et al., 2001). Based on a number of reports implicating VEGF in the development of human PAH, the authors hypothesized that the inhibition of VEGFR2, the receptor tyrosine kinase for VEGF, could prevent PH induced by CH (Taraseviciene-Stewart et al., 2001). To inhibit VEGFR2 the authors utilized SU5416, a potent and selective inhibitor of VEGFR2 (O'Donnell et al., 2005), originally designed as a small molecule inhibitor of angiogenesis to be used in the treatment of human solid tumours (Hoff et al., 2006). Paradoxically, rather than being beneficial, SU5416-mediated inhibition of VEGFR2 markedly increased RVSP and RVH (Taraseviciene-Stewart et al., 2001). Furthermore, medium sized and pre-capillary intra-alveolar arterioles of SU/CH rats showed near-complete lumen obliteration and extensive EC proliferation (Taraseviciene-Stewart et al. 2001). Since this initial report, it has been shown that these pathohistological features are virtually identical to those seen in human PAH (Abe et al., 2010). While Taraseviciene-Stewart and colleagues proposed that initial widespread EC death combined with hypoxia resulted in the selection of apoptosis-resistant and highly proliferative ECs, this proliferative hypothesis has never been adequately proven. In any case, in comparison to other available animal models, it appears that the SU/CH model may best recreate the pathogenesis, progression, and

characteristics of severe human PAH, and thus, is considered to be the model of choice by many investigators in the field.

1.1.4.5 The Proliferative Hypothesis of PAH

As first described by Rubin Tuder, the proliferative hypothesis of PAH proposes that widespread EC apoptosis results in the selection of hyperproliferative, apoptosis-resistant pulmonary ECs which contribute to complex vascular remodelling and the formation of plexiform lesions (Tuder et al., 1994). While the ability to directly test this hypothesis is greatly restricted by our limited access to early stage PAH tissues, evidence of monoclonal EC growth and microsatellite instability has been observed in the plexiform lesions of patients with PAH (Lee et al., 1998; Yeager et al., 2001). Furthermore, primary ECs isolated directly from the lungs of patients with advanced PAH display a hyperproliferative, apoptosis-resistant phenotype in culture (Masri et al., 2007). Immunohistochemical analyses of complex concentric arterial lesions in the lungs of SU/CH rats also indicate abnormal EC growth as evidenced by the expression of angiogenesis-related molecules such as VEGFR2, hypoxia-inducible factor 1-alpha (HIF-1α) (Tuder et al., 2001), and cell adhesion molecule CD44 (Ohta-Ogo et al., 2012).

Given the suspected role of growth-dysregulated ECs in the genesis of plexiform lesions, parallels between cancer and PAH have been suggested (Rai et al., 2008). In line with the so-called “cancer paradigm” of PAH, cells associated with plexiform lesions and complex vascular remodelling display characteristics that are typical of human cancer cells such as angiogenesis, evasion of apoptosis, and insensitivity to growth signals (Rai et al., 2008). Reduced expression of pro-apoptotic proteins and increased expression of

survival factors, such as the protein survivin, have also been reported in ECs from patients with IPAH (McMurtry et al., 2005). Moreover, a study comparing vascular lesions in patients with "reversible" or "irreversible" PH associated with congenital heart disease found that the anti-apoptotic protein Bcl-2 was exclusively expressed by ECs associated with arteries displaying severe intimal fibrosis in patients with irreversible PH (Levy et al., 2007).

In addition to an increased resistance to apoptosis, other groups have reported that vascular cells involved in the formation of complex vascular lesions in PAH may have an impaired ability to respond to DNA damage. Recently, de Jesus Perez and colleagues demonstrated that the vascular lesions of IPAH patients have low levels of DNA topoisomerase 2-binding protein 1 which is involved in responding to DNA damage and repair (de Jesus Perez et al., 2014). This finding is in keeping with earlier reports demonstrating minimal expression of the tumour suppressor protein p27 in the core region of plexiform lesions from patients with severe PAH (Cool et al., 1999). Complimentary *in vitro* studies have shown that pulmonary ECs derived from IPAH patients, or HPAH patients with *Bmpr2* mutations, are highly susceptible to DNA damage compared to control cells (Li et al., 2014). Collectively, these findings suggest that an inability to repair and respond to DNA damage may be another potential mechanism underlying the emergence of growth-dysregulated ECs in PAH.

1.1.4.6 The Degenerative Hypothesis of PAH: The Role of EC Apoptosis

Collectively, evidence from patient samples and pre-clinical experimental animal models all point to a central role for EC apoptosis in "triggering" the pathogenesis of PAH (Jurasz et al., 2010). In addition to triggering the emergence of growth-dysregulated ECs, as discussed in the previous section, it is possible that widespread EC apoptosis at the level of the pre-capillary arteriole may lead to extensive microvascular degeneration and dropout (Jurasz et al., 2010). Rat models have been instrumental in improving our understanding of how EC apoptosis may contribute to microvascular degeneration. Through detailed studies of the MCT rat model, our group has identified marked EC apoptosis at the level of the pre-capillary arteriole as early as three days following MCT injection as evidenced by terminal deoxynucleotidyl transferase dUTP nick end labeling (TUNEL) (Zhao et al., 2005). Compared to controls, the lungs of rats injected with MCT show a time-dependent increase in TUNEL staining which correlates with increases in RVSP (Zhao et al., 2005). Most notably, rats injected with MCT have a marked loss of microvascular perfusion and widespread pre-capillary occlusion as revealed by fluorescent microangiography (Zhao et al., 2005). Our group has also made similar observations in the SU/CH rat model of PAH (Jiang et al., 2015). Following 1 week of SU/CH, rat lungs display increases in caspase-3 staining that is associated with arteriolar endothelium. Moreover, whole lung lysate immunoblotting revealed a significant increase in activated caspase-3 in SU/CH rats compared to normal controls (Jiang et al., 2015).

At present, the relative contribution of proliferative and degenerative changes on the overall loss of pulmonary microcirculation is not known, however, the former has attracted the greatest amount of interest in the field by far. At present, there appears to be

no conflict between the "degenerative" paradigm and the "proliferative" paradigm, and indeed, it is likely that both of these processes contribute to the loss of effective lung microcirculation in the disease.

1.1.4.7 Inflammation in PAH

In PAH patients and experimental animal models inflammatory cell infiltrates such as macrophages, mast cells, T- and B-lymphocytes and dendritic cells, are commonly observed in the adventitial layer of remodelled vessels (Archer et al., 2010; Stacher et al., 2012; Tuder et al., 1994). Evidence suggests that inflammatory cells contribute to vascular remodelling by releasing a variety of cytokines, chemokines, and growth factors (Price et al., 2012). Once released, these inflammatory signals may induce the proliferation, necrosis, or differentiation of nearby non-inflammatory cells such as pulmonary ECs and smooth muscle cells. Additionally, these signals may attract other immune and/or inflammatory cells to participate in processes such as tissue repair (Price et al., 2012). Inflammatory cells such as macrophages, dendritic cells, and mast cells have also been implicated in the remodelling of pulmonary vessels in both the MCT and SU/HX rat models of PAH (Dahal et al., 2011; Savai et al., 2012; Otsuki et al, 2015).

1.1.5 Translationally Controlled Tumour Protein (TCTP) in PAH

Understanding the cellular and molecular mechanisms contributing to the hyperproliferative, apoptosis-resistance phenotype of pulmonary ECs in PAH remains a key area of ongoing PAH research. From a pathobiological perspective, such mechanisms could provide essential insight into the complex nature of PAH development and

potentially lead to the identification of early PAH prognostication markers. Alternatively, from a therapeutic standpoint, a greater understanding of the mechanisms underlying the development of PAH could spur the development of specific therapeutic approaches targeting complex vascular remodelling. Unfortunately, our ability to analyze these mechanisms has been severely limited by the scarcity of patient material from early stage PAH. In order to circumvent this shortcoming, our group turned our attention to blood-outgrowth endothelial cells (BOECs), an alternative source of human endothelial-like cells that can be readily isolated from whole blood (Asahara et al., 1997; Ingram et al., 2005). Also termed late outgrowth endothelial progenitor cells, or endothelial colony forming cells, BOECs are derived from peripheral blood mononuclear cells in long-term (>2 weeks) culture. These extensively characterized cells exhibit a strong EC phenotype that is nearly identical to mature ECs (Ingram et al., 2004).

By combining a high-throughput two-dimensional polyacrylamide gel and mass spectrometry proteomic approach, Dr. Jessie Lavoie, a former doctoral candidate in our lab, compared the proteomic profiles of BOECs from HPAH patients with known *Bmpr2* mutations to BOECs from healthy aged-matched controls (Lavoie et al., 2014). Subsequent analysis identified 22 proteins that were significantly dysregulated in HPAH patient cells (11 up-regulated and 11 down-regulated), of which TCTP was selected for further analysis based on its previously reported role in malignant transformation, proliferation, inflammation, and cancer cell survival (Amson et al., 2013; MacDonald et al., 1995; Tuynder et al., 2004; Tuynder et al., 2002).

Our lab went on to confirm that TCTP levels were significantly elevated in HPAH BOECs compared to controls via immunoblotting. Immunofluorescence staining of

HPAH lung sections revealed that TCTP was closely associated with the EC marker CD31 in complex vascular lesions. *In vitro,* knockdown of TCTP in HPAH and control BOECs using small interfering RNAs (siRNA) resulted in a marked reduction in proliferation and increased the percentage of early-stage apoptotic cells in HPAH BOECs only; in effect reversing the pathological phenotype. siRNA-mediated knockdown of BMPR2 in BOECs resulted in increased TCTP expression and a significant reduction in mir27b levels. Mir27b has been previously implicated in human PAH and has also been shown to negatively regulate TCTP in the context of oral cancer (Drake et al., 2011; Lo et al., 2012). Furthermore, mir-27b has also been found to be involved in the shear-stress dependent recruitment of pericytes and stabilization of newly formed blood vessels by down-regulating angiopoietin 2 and semophorin A6 (Demolli et al., 2013).

In vivo, lung sections from rats injected with SU5416 displayed TCTP immunoreactivity in the perivascular adventitia and intima of remodelled arterioles. However, TCTP immunoreactivity did not correspond to staining for pulmonary smooth muscle cells. Further immunofluorescence staining revealed that TCTP also corresponded with actively proliferating cells and monocytes/macrophages as evidenced by proliferating cell nuclear antigen (PCNA) and CD68 staining, respectively.

1.1.5.1 TCTP: A Link Between EC Apoptosis and Dysregulated Vascular Cell Growth in PAH?

Collectively, our findings implicate TCTP as a "missing link" between EC apoptosis, EC dysfunction, inflammation, and complex vascular remodelling in human PAH. Interestingly, another group has previously reported a link between TCTP, EC

apoptosis, and vascular cell survival/proliferation (Sirois et al., 2011). In 2011, Sirois and colleagues performed a proteomic analysis of exosome-like nanovesicles released from apoptotic ECs to identify proteins involved in inducing resistance to apoptosis in neighbouring vascular cells (Sirois et al., 2011). In their report, the authors noted that TCTP was markedly enriched in nanovesicles released from apoptotic ECs in a caspase-dependent manner (Sirois et al., 2011). The authors went on to show that apoptotic EC conditioned media promoted smooth muscle cell survival after serum withdrawal and that this effect was mediated by nanovesicles containing TCTP (Cho et al., 2012; Sirois et al., 2011). Although, these findings were in the context of systemic arterial injury and remodelling, they provide credence to the concept of TCTP as a potent survival factor that can be released by ECs undergoing apoptosis. In regards to PAH, the release of TCTP by pulmonary ECs undergoing apoptosis may be a mechanism by which TCTP facilitates the emergence of growth-dysregulated lung vascular cells involved in the formation of plexiform lesions and complex vascular remodelling.

1.2 What is TCTP?

1.2.1 General Overview

TCTP, also known as Q23, fortilin, and histamine releasing factor (HRF), is a ubiquitous, highly networked, and evolutionarily conserved protein that has been shown to be involved in processes such as cell cycle regulation, DNA processing/repair, protein/RNA biogenesis, and cell survival (Amson et al., 2013; Li et al., 2001; MacDonald et al., 1995; Thomas et al., 1981). The regulation of TCTP is influenced by a variety of intracellular and extracellular cues. For example, environmental stress, growth signals, developmental/tissue-specific factors, cytokines, and pro-apoptotic stimuli have

all been shown to impact TCTP regulation (Bommer & Thiele, 2004). While TCTP overexpressing mice develop systemic arterial hypertension at around six weeks of age (Kim et al., 2008), TCTP-null mice are embryonic lethal due to widespread apoptosis during development and display evidence of BMP pathway over-activation (Koide et al., 2009). In regards to PAH, this may suggest that TCTP exerts an inhibitory regulatory role over this critical pathway and that its overexpression in the lung vasculature could further reduce BMP signalling, a potential additional mechanism for inducing complex vascular remodelling in PAH.

1.2.2 TCTP in Inflammation

In 1995, a novel pro-inflammatory role for TCTP as an IgE-dependent histamine releasing factor was identified from studies investigating allergic responses and non-resolving inflammation in asthma (MacDonald et al., 1995). In the context of atherosclerosis, TCTP has been shown to participate in disease progression by increasing the longevity of macrophages found in atherosclerotic plagues (Pinkaew et al., 2013). In regards to allergy and asthma, TCTP has been shown to stimulate cytokine production from IgE-sensitized basophils and mast cells and TCTP-activities have been found in bodily fluids during late phase allergic reactions (Kashiwakura et al., 2012). While our initial report on TCTP in PAH provided some evidence to support a monocyte/macrophage connection, the role of TCTP in mediating the chronic inflammatory response in PAH requires further investigation.

1.2.3 TCTP in Cell Growth, Survival, Apoptosis & Cancer

Although TCTP may be an important mediator of non-resolving inflammation, the protein is best known for its role in cancer. Several studies have implicated TCTP in the process of malignant transformation and as a mediator of cancer cell proliferation and survival (Li et al., 2001; Telerman & Amson, 2009; Tuynder et al., 2002). On the molecular level, investigations into the process of tumour reversion have also identified TCTP as a keystone regulator of the MDM2-p53 axis (Amson et al., 2012). TCTP prevents the auto-ubiquitination of MDM2 (murine double minute 2), an E3 ubiquitin ligase, thereby promoting MDM2-mediated ubiquitination and transcriptional inhibition of p53 (Amson et al., 2012). Accordingly, two small molecules, sertraline and thioridazine, have been shown to directly bind TCTP *in vitro* and neutralize its activation of the MDM2-p53 axis thereby promoting p53 stabilization and TCTP degradation (Amson et al., 2012). Of note, pharmacological inhibition of MDM2 with the anti-cancer drug Nutlin3a was recently shown to be an effective "pro-senescence" treatment for PAH by preventing pulmonary artery smooth muscle cell proliferation in mice (Mouraret et al., 2013).

TCTP may also prohibit apoptosis by antagonizing the pro-apoptotic activity of Bax (Susini et al., 2008). During intrinsic apoptotic signalling, Bax dimerization induces the release of cytochrome c from the mitochondria following dimerization and aggregation on the mitochondrial membrane. Structurally, the H2–H3 helices of TCTP and the H5–H6 helices of Bax share a high degree of similarity (Susini et al., 2008). *In vitro* experimental evidence suggests that these structural similarities allow TCTP to antagonize apoptosis by inserting into the mitochondrial membrane and inhibiting Bax

dimerization (Susini et al., 2008). TCTP has also been shown to inhibit the amplification of mitochondrial-mediated apoptotic signalling in HeLa cells by interacting with the caspase recruitment domain of Apaf-1 in the apoptosome (Jung et al., 2014).

1.2.4 TCTP Small Molecule Inhibitors

1.2.4.1 Thioridazine

Thioridazine, formerly marketed under the name Mellaril, was an antipsychotic drug prescribed for the treatment of schizophrenia, psychosis, and dementia (Kirchner et al., 2001). In 2005, thioridazine was withdrawn worldwide amid reports of severe cardiovascular side effects such as prolonged QT interval and torsades de pointes (Stollberger et al., 2005). A member of the phenothiazine drug group, thioridazine exerts its primary therapeutic effects by reducing dopaminergic neural transmission via D2 dopamine receptor blockade (Seeman, 1990). In addition to the D2 dopamine receptor, thioridazine has a high binding affinity for other dopamine receptors, D_1, D_3, D_4; acetylcholine receptors, M_1, M_3, M_5; serotonin receptors, 5-$HT_{2A,}$ 5-HT_{2C}; histamine receptor H_1; and the androgenic receptors alpha-1a and alpha-1b (Roth et al., 2011).

The first report demonstrating the ability of thioridazine to down-regulate TCTP was published in 2004 by Tuynder and colleagues (Tuynder et al., 2004). Citing the role of TCTP as a histamine releasing factor, the authors hypothesized that other compounds with the ability to inhibit the histaminic pathway might also antagonize the function of TCTP. While none of their initial test compounds proved to be successful, structurally related molecules, namely thioridazine and sertraline, effectively reduced TCTP levels and induced apoptosis in U937 human leukemia cells (Tuynder et al., 2004). In a follow-

up report published in Nature Medicine, the same group performed surface plasmon resonance to demonstrate that both thioridazine and sertraline bind directly to TCTP and inhibit the function of the protein (Amson et al., 2012).

Thioridazine has two enantiomers that are both metabolized by the liver enzyme CYP2D6 into (S)- and (R)-thioridazine 2-sulfoxide, also known as mesoridazine (Eap et al., 1996). In humans and rats, the mean urinary excretion time of thioridazine and its metabolites ranges between 24 and 48 hours (Lin et al., 1993). In the literature, thioridazine is typically administered at a dose of 10 mg/kg/day to achieve pharmacological effects in rats (Haduch et al., 2007; Maj et al., 1979; Shi et al., 2012; Wojcikowski & Daniel, 2002). Thus, this dose served as a benchmark for the experiments contained within this thesis.

1.2.4.2 Sertraline

Sertraline is a commonly prescribed tri-cyclic anti-depressant belonging to the selective serotonin reuptake inhibitor (SSRI) class. Like other SSRIs, sertraline's effectiveness in the treatment of depression is presumed to come from its ability to bind serotonin transporters (SERT) and inhibit neuronal serotonin re-uptake, thereby maintaining extracellular concentrations of serotonin (Yildiz et al., 2002). In humans, sertraline has an estimated elimination half-life of 22-37 hours and is metabolized primarily by hepatic CYP-oxidation (Murdoch & McTavish, 1992). The main serum metabolite of sertraline is N-desmethylsertraline, a far less potent serotonin reuptake inhibitor with estimated half-life of 71-206 hours (Ludmark et al., 2000). In rats, the elimination half-life of sertraline is approximately 3.55-4.5 hours (Melis et al., 2012).

In contrast to thioridazine, sertraline has been the explored as a therapy for PAH in the MCT rat model (Li et al., 2006). In 2006, Li and colleagues reported that sertraline, administered at a dose of 10 mg/kg/d by oral gavage for three weeks, could protect rats against MCT-induced PH as evidenced by significantly decreased RVSP and RVH compared to vehicle control rats. The authors went on to show that sertraline significantly decreased the number of "fully muscularized" pulmonary vessels and decreased pulmonary artery SERT mRNA expression compared to controls (Li et al., 2006). Although the authors did not analyze the effect of sertraline on TCTP, their report provides data to support further evaluating sertraline in the SU/CH rat model of experimental PAH.

OBJECTIVES & HYPOTHESES

2.1 Objectives

1. To explore TCTP as a potential therapeutic target for PAH by determining the effects of putative small molecule TCTP inhibitors (thioridazine or sertraline) on:
    a. Growth and survival of rat lung microvascular endothelial cells (RLMVECs) *in vitro* and;
    b. Pulmonary hemodynamics, right ventricular remodelling, and arterial remodelling in the SU/CH rat model of severe PAH *in vivo.*
2. To further investigate the role of TCTP in pulmonary vascular remodelling and inflammation *in vivo* using the SU/CH rat model.

2.2 Hypotheses

2.2.1 General Hypothesis

TCTP represents a central molecular mechanism linking EC damage and apoptosis to the emergence of growth-dysregulated lung vascular cells and occlusive, complex arterial remodelling in PAH.

2.2.2 Specific Hypotheses

1. Inhibition of TCTP *in vitro* using putative small molecule TCTP inhibitors will down-regulate TCTP in RLMVECs and increase their susceptibility to apoptosis.
2. Inhibition of TCTP *in vivo* using small molecule TCTP inhibitors will reduce RVSP improve right ventricle remodelling in the SU/CH model rat model.

3. Regardless, of their overall effect on pulmonary hemodynamics, inhibition of TCTP *in vivo* using small molecule TCTP inhibitors will inhibit the progression of PAH in SU/CH rat model by preventing complex arterial remodelling and inflammation in the lung.
4. TCTP will co-localize with inflammatory cells, such as macrophages, surrounding vascular lesions in the SU/CH rat model of PAH.

METHODS & MATERIALS

3.1 In Vitro

3.1.1 RLMVEC Cell Culture

Commercially available primary neo-natal rat lung microvascular endothelial cells (RLMVECs) isolated from Sprague Dawley rats (R1066, Cell Biologics) were used for all *in vitro* experiments. RLMVECs were cultured in complete growth media (M1266, Cell Biologics) and maintained at 37°C in 5% CO_2. Cells were only used between the 4^{th} and 9^{th} passages. Cell viability was assessed by 0.4% trypan blue exclusion (Countess®, Life Technologies).

3.1.2 Annexin V/7AAD Assay & Flow Cytometry

$4.5x10^4$ RLMVECs were plated in 2 mL of complete growth media in each well of a 6 well plate. The following day the media was removed and replaced with fresh media containing 5, 10, or 20 μM thioridazine. 750 nM staurosporine (STS; S5921, Sigma-Aldrich) was used as a positive control for apoptosis. A vehicle control well was also prepared containing 0.1% DMSO in complete media. After 24 hours, the media was aspirated and the cells were washed twice in PBS. To lift adherent cells, TrypLE Express (12604013, Life Technologies) was added to each well and plates were incubated at 37°C for 10 minutes. Annexin V/7AAD staining was performed using the Violet Annexin V/Dead Cell Apoptosis Kit with Pacific Blue™ Annexin V/SYTOX® AADvanced™ according to the manufacturer's instructions (A35136, Life Technologies). Once stained, the cells were analyzed using the Attune® Auto Sampler (Life Technologies). The resulting flow cytometry data was analyzed using FlowJo (version 10.0.7, FlowJo LLC).

3.1.3 Caspase 3/7 Activity Assay

$3x10^6$ RLMVECs were plated in 100 µl of complete growth media in each well of a 96 well plate. The following day the media was removed and replaced with fresh media containing 5, 10, or 20µM thioridazine. 750nM staurosporine (STS; S5921, Sigma-Aldrich) was used as a positive control for apoptosis. 0.1% DMSO was used as a vehicle control. After 24 hours, caspase 3/7 activity was determined using the Apo-ONE® Homogeneous Caspase-3/7 Assay (G7792, Promega). In accordance with the manufacturer's instructions, pro-fluorescent Apo-ONE® Caspase-3/7 reagent was prepared by combining Z-DEVD-R110 [rhodamine 110, bis-(N-CBZL-aspartyl-L-glutamyl-L-valyl-L-aspartic acid amide] substrate and permeabilization buffer. The pro-fluorescent reagent was then added to each well and incubated at room temperature for 1 hour. During the incubation period cells with active caspase 3/7 sequentially cleave DEVD peptides from the Z-DEVD-R100 substrate producing highly fluorescent rhodamine 110. Following incubation, rhodamine 100 fluorescence was assayed using the BioTek Synergy HT plate reader (BioTek).

3.1.4 Cell Lysate Preparation

$2x10^5$ RLMVECs were plated in 10mL of complete growth media in each well of a 6 well plate. The following day the media was removed and replaced with fresh media containing 5, 10, or 20 µM thioridazine. 0.1% DMSO was used as a vehicle control. After a 24 hour incubation, the media was aspirated and the cells were washed twice in PBS. To lift the cells, TrypLE Express (12604013, Life Technologies) was added to each well and the plates were incubated at 37°C for 10 minutes. Cells were counted by 0.4% trypan

blue exclusion and then pelleted by centrifugation at 400XG for 4 minutes. The supernatant was aspirated and the remaining cell pellet was suspended in RIPA buffer containing protease inhibitors (04693116001, Roche). Additional lyses steps, protein quantification, and immunoblotting was performed as described below.

3.2 In Vivo

3.2.1 Experimental Design

In order to assess the effects of the TCTP small molecule inhibitors on TCTP abundance and the development of PAH *in vivo* we utilized the SU/CH rat model. In an effort to parallel treatment in a clinical setting, the delivery of the TCTP small molecule inhibitors was delayed until the development of experimental PAH at the end of week 4. Direct measurements of RVSP and histological analyses of the pulmonary vasculature were used to confirm the development of PAH and vascular remodelling at this time point. Prior to the delivery of TCTP small molecule inhibitors, rats were block randomized into three groups: thioridazine (Thio; 10 mg/kg/d), sertraline (Sert; 10mg/kg/d), or vehicle control (Vehicle; 25% DMSO/75% PEG). Randomization was accomplished using open-access randomization software available online at www.randomization.com. Small molecule TCTP inhibitors were continuously delivered for three consecutive weeks (i.e. week 4 to the end of week 7) via subcutaneous osmotic mini-pumps. One day prior to the experimental endpoint at the end of week 7, rats underwent transthoracic echocardiography to assess cardiac function. The next day, a second RVSP measurement was performed and lung tissues were collected for subsequent analyses (Figure 2).

3.2.2 Animals & SU/CH Rat Model of PAH

All animal procedures were approved by the University of Ottawa Animal Care Committee and adhered to the guidelines of the Canadian Council on Animal Care. Male Sprague-Dawley rats (n=44; ~125g) (Harlan Labs, Indianapolis, Indiana) were injected with a single subcutaneous bolus of SU5416 [3-(3,5-dimethyl-1H-pyrrol-2-ylmethylene)-1,3-dihydroindol-2-one] (20mg/kg) (3037, Tocris, Bristol) suspended in a vehicle of CMC (0.5% carboxymethylcellulose sodium, 0.9% sodium chloride, 0.4% Tween 80, 0.9% benzyl alcohol in deionized water) (Sigma-Aldrich). Immediately following SU5416 injection, rats were placed in hypoxic chambers (~10 O_2) for 3 weeks. At the end of the week 3, rats were removed from the hypoxic chambers and recovered in normoxia for 1 week before small molecule delivery. During exposure to chronic hypoxia rats were housed 3 per cage. After removal from hypoxia, rats were housed 2 per cage. Throughout the entire 7 weeks all rats were maintained on a light–dark (12 hour/12 hour) cycle and received water and food *ad libitum.*

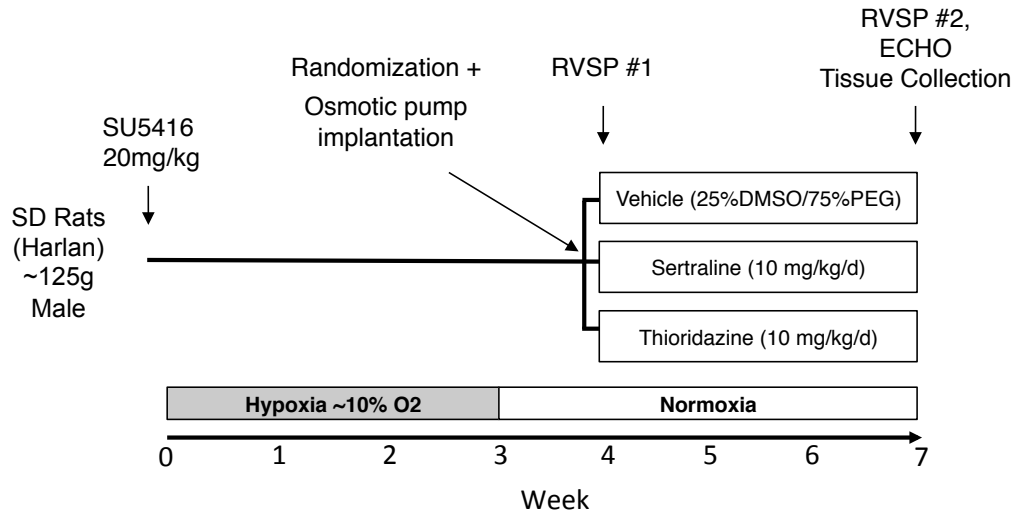

Figure 2. Experimental design for sertraline and thioridazine delivery in the SU/CH rat model of PAH.

3.2.3 Right Ventricular Catheterization

To determine baseline and endpoint measurements of RVSP, right ventricle catheterization was performed at end of week 4 and at the end of week 7, respectively. Prior to each intervention, rats were anesthetized by a single intraperitoneal injection of ketamine (35 mg/kg) and xylazine (7 mg/kg). Using aseptic surgical techniques, the right jugular vein was exposed and a high-fidelity pressure catheter (Transonic-Sciscene Inc.) was advanced through the superior vena cava into the right ventricle of the heart. Correct catheter placement was determined by observing pressure tracings prior to data collection. Hemodynamic parameters were analyzed using the LabScribe2 software (iWorx). RVSP data was collected and analyzed by a blinded experimenter.

3.2.4 Small Molecule Preparation & Osmotic Pump Implantation

Both sertraline (S6319, Sigma-Aldrich) and thioridazine (T9025, Sigma-Aldrich) were dissolved in a solution of 25% DMSO (D2438, Sigma Aldrich) and 75% PEG (202398, Sigma Aldrich). Once dissolved, the solutions were loaded into osmotic mini-pumps (2ML4, Alzet Osmotic Pumps) according to the manufacturer's instructions to achieve a delivery rate of 10 mg/kg/d.

3.2.5 Transthoracic Echocardiographic Evaluation

One day prior to the week 7 experimental endpoint, right ventricle structure and function was assessed using non-invasive transthoracic echocardiography (Vevo 2100, VisualSonics) (Tei et al., 1996). Anesthesia was induced using vaporized isoflurane delivered to effect at a concentration of 5% and maintained at 1.5-2% in oxygen (~2

ml/minute). To determine pulmonary arterial acceleration time (PAAT), the transducer was aligned with the pulmonary artery (PA) in the parasternal short-axis view and pulmonary outflow was recorded using the pulse-wave Doppler mode. From the resulting pulmonary arterial waveform, PAAT was measured as the time from the initiation of systolic flow to peak outflow velocity. Measurements of CO and stroke volume (SV) were indirectly determined using PA diameter, PA velocity time integral (VTI) and heart rate (HR) according to a previously described method (Urboniene et al., 2010). To perform structural measurements of the right and left ventricles (i.e. right ventricle internal diameter (RVID) and left ventricle internal diameter (LVID)), parasternal short-axis echocardiographic images were collected in M-mode. Right ventricle free wall thickness (RVfWT) was measured as the distance between the epicardium and the endocardium of the right ventricular wall. Tricuspid annular plane systolic excursion (TAPSE) was measured as tricuspid annular movement from end-diastole to end-systole using an apical 4-chamber view in M-mode. Echocardiographic data was collected and analyzed by a blinded experimenter.

3.2.6 Assessment of Right Ventricle Hypertrophy (RVH)

Immediately following excision at the experimental endpoint, each heart was prepared for sectioning by removing the atria and pulmonary trunk. A blinded experimenter sectioned each heart into three parts: the right ventricle, the left ventricle, and the septum. RVH index was calculated as right ventricle mass divided by left ventricle mass plus septum mass (RV/LV+S).

3.2.7 Rat Lung Isolation and Paraffin-embedding

After measuring hemodynamic parameters at the week 7 experimental endpoint, the left lung was insufflated via the trachea with a 50% OCT - 50% saline solution (Tissue-Tek OCT; Qiagen) and removed. The removed lung was then sectioned transversely into five discrete pieces. Two non-adjacent pieces were then fixed in a 4% paraformaldehyde solution overnight at 4°C. The following day, the fixed lung sections were rinsed in PBS and stored for approximately 1-2 weeks in 70% ethanol until they were dehydrated in alcohol and embedded in paraffin blocks. Using a microtome (Leica Microsystems), 5µm sections were cut from the paraffin blocks, mounted onto poly-L-lysine coated slides, and dried overnight at 37°C.

3.2.8 Pulmonary Vessel Obliteration & Adventitial Cell Clearance

To assess pulmonary vessel obliteration and adventitial remodelling SU/CH rat lung sections were stained with hematoxylin and eosin (H+E) to visualize lung morphology. Slides were imaged using a Panoramic DESK slide scanner (3DHistech Ltd.) and analyzed using the Panoramic Viewer software (3DHistech Ltd.). For the assessment of both pulmonary vessel obliteration and adventitial cell clearance, a blinded experimenter scored 100 vessels (<150µm in diameter) per rat (i.e. 50 vessels per transverse cross-section). Pulmonary vessel obliteration was scored using the criteria outlined in Table 2. To assess adventitial cell clearance, pulmonary vessels (<150µm in diameter) were classified as having either evidence of adventitial cell clearance or no evidence. Adventitial cell "clear zones" were defined as acellular space, of any size, in the adventitial layer (Figure 12).

Table 2. Pulmonary vessel obliteration classification criteria.

Classification	Criteria
None	• Lumen is fully visible and easily identifiable • Medial layer is easily identifiable in medium-to-large vessels. • No evidence of intimal hypertrophy/hyperplasia • Little to no evidence of adventitial/perivascular cell accumulation
Partial	• Lumen is partially obstructed and more difficult to identify upon initial inspection • Medial layer is more difficult to identify for medium-to-large vessels • Some evidence of intimal hypertrophy/hyperplasia. • Some evidence of adventitial/perivascular cell accumulation
Complete	• Complete luminal obliteration (i.e. the lumen is fully obstructed and no longer identifiable) • Medial layer is difficult or impossible to identify upon initial inspection • Clear intimal hypertrophy/hyperplasia evident. • Marked adventitial/perivascular cell accumulation

Adapted from Farkas D et al., 2014.

3.2.9 Immunofluorescence & Immunohistochemistry

For immunofluorescence staining, all paraffin-embedded rat lung sections were first de-waxed and dehydrated through graded alcohols. Slides were then quenched in a 0.1 M glycine solution for 15 minutes to block auto-fluorescence. Antigen retrieval was performed by submerging slides into near-boiling sodium citrate buffer

(0.4 mol/L) at pH 6.0 (H-3300, Dako) for a total of 30 minutes. After cooling to room temperature, slides were permeabilized in 0.25% triton-X100 for 10 minutes. A blocking solution consisting of 3% bovine serum albumin (9998, Cell Signalling Technology) and 5% goat serum (5425S, Cell Signaling Technology) was applied for 60-90 minutes at room temperature before slides were incubated with primary antibodies. The following primary antibodies were incubated overnight at 4°C: polyclonal rabbit anti-TCTP (ab37506, Abcam), mouse monoclonal anti-rat monocytes/macrophages (CD68) (MAB1435, Millipore). Alternatively, monoclonal mouse anti-α-smooth muscle actin (α-SMA)-Cy3 (C6198, Dako) antibody was incubated 1 hour at room temperature. TCTP and CD68 primary antibody specificity was demonstrated by the following isotype controls used at the same concentration as the corresponding primary antibody: mouse (G3A1) mAb IgG1 isotype control (5415, Cell Signalling Technology) (for CD68) and rabbit IgG isotype control (NB810-56910, Novus Biologicals) (for TCTP) (Supplemental Figure 1). Corresponding secondary antibodies were incubated for 1 hour at room temperature: Alexa Fluor® 555 goat anti-nouse IgG (H+L) (A21422, Invitrogen) (for CD68), Alexa Fluor® 488 goat anti-rabbit IgG (H+L) (A11008, Invitrogen) (for TCTP). Images were acquired with the Zeiss Axio Imager M2 Microscope (Carl Zeiss Microscopy) using a 20X objective. TCTP immunohistochemistry was performed at the

University of Ottawa's PALM Histology Core Facility. Polyclonal rabbit anti-TCTP (ab37506, Abcam) was used as the primary antibody (Supplemental Figure 2).

3.10 Lung Collection, Homogenization & Immunoblotting

Immediately following excision, the right lung was snap frozen in liquid nitrogen and stored at -80°C until use. For each rat, 50 mg of tissue was homogenized in RIPA buffer (20-188, Merek Millipore) spiked with protease inhibitors (04693116001, Roche) and lysed using the TissueLyser II (Qiagen). Lysates were sonicated and then centrifuged for 7 minutes at 12500 RPM (4°C) to remove cellular debris. Following the spin, the supernatant was collected and stored at -80°C. An in-house bicinchoninic acid assay was performed to determine protein concentrations. All immunoblotting steps, including sample preparation, were performed according to the manufacture's instructions (Novex® nupage® SDS-PAGE Gel System, Life Technologies). A total of 12 µg of sample protein was loaded per lane and run at 150 volts for 70 minutes on 4-12% Bis-Tris Gel (NP0335PK2, Life Technologies). A dry transfer was performed using the iBlot ® Dry-transfer System (Life Technologies) onto nitrocellulose membranes (IB301001, Life Technologies). Membranes were subsequently blocked with TBS-T 5% milk for 1-1.5 hours. Immediately after, membranes were probed overnight at 4°C with the following primary antibodies prepared in TBS-T with 5% milk: anti-rabbit TCTP polyclonal (1:500; Ab37506, Abcam) and anti-mouse β-actin monoclonal (1:15000; A5441, Sigma-Alderich). The following day, membranes were probed with the corresponding IRdye infrared secondary antibodies for 1 hour at room temperature and imaged using the Li-COR Odyssey Infrared Imaging System (Li-Cor Biosciences).

3.3 Statistical Analyses

Unless stated otherwise, statistical analyses of the data were performed using unpaired, two-tailed Student's t-tests or ordinary one-way ANOVAs followed by a post-hoc Dunnet test to correct for multiple comparisons. All analyses were performed using GraphPad Prism (Version 6, GraphPad Software, Inc.). Statistical significance was accepted at $p<0.05$.

RESULTS

4.1 In Vitro

4.1.1 Thioridazine Decreases RLMVEC Viability

RLMVECs exposed to thioridazine for a period of 24 hours showed a dose-dependent decrease in viability as determined by 0.4% trypan blue exclusion (Figures 3A & 3B). Morphologically, RLMVECs exposed to higher concentrations of thioridazine (10 and 20 μM) appeared to display apoptosis-like characteristics (Figure 3C). This suggested that thioridazine reduced RLMVEC viability through the initiation of apoptosis.

4.1.2 Thioridazine Induces Hallmarks of Apoptosis in RLMVECs

As evidenced by flow cytometry, 24 hour thioridazine exposure resulted in a dose-dependent increase in the proportion of early apoptotic RLVMECs (annexin V+/7AAD-) (Figure 4C). This was accompanied by a dose-dependent decrease in the proportion of viable RLMVECs (annexin V-/7AAD-) (Figure 4B). Furthermore, 20 μM thioridazine significantly increased the proportion of necrotic RLMVECs (7AAD+), indicating that thioridazine is likely cytotoxic at higher concentrations ($p<0.05$) (Figure 4D). In a separate assay, RLMVECs exposed to increasing concentrations of thioridazine for a period of 24 hours displayed a dose-dependent increase in caspase 3/7 activity (Figure 5). However, this increase was only significant at 20 μM thioridazine ($p<0.05$) (Figure 5).

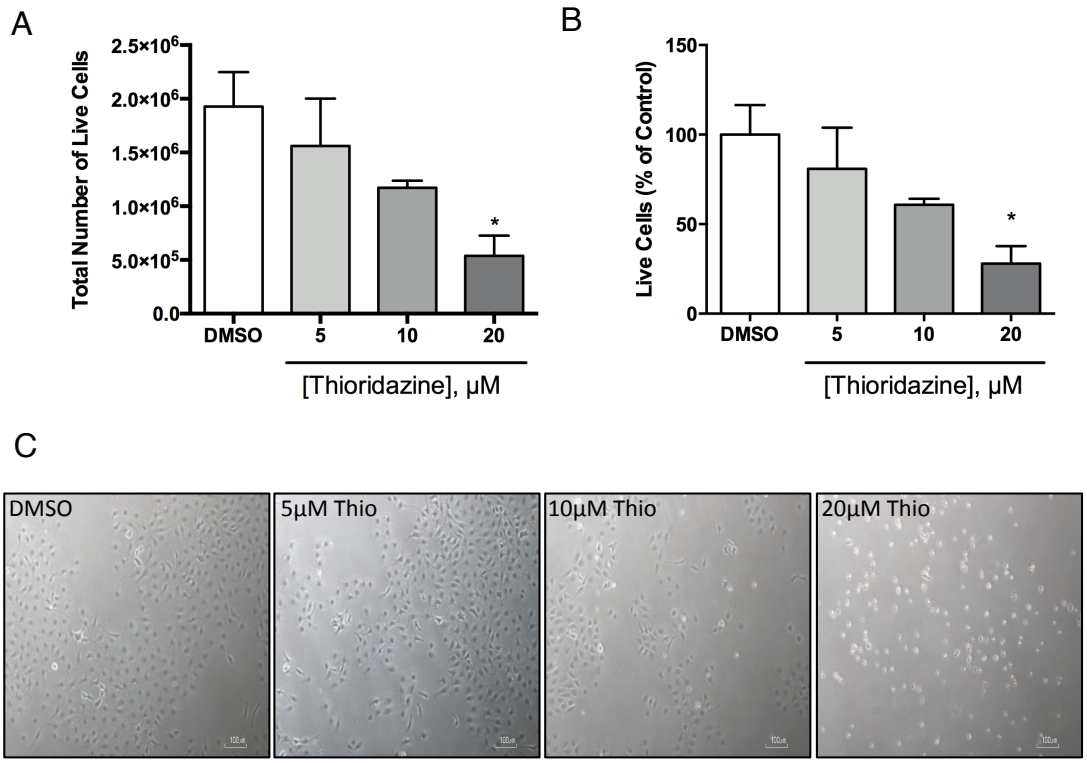

Figure 3. **Thioridazine dose-dependently decreases RLMVEC viability after 24 hours. A**. 20 µM thioridazine significantly reduces the total number of viable RLMVECs after 24 hours. **B**. 20 µM thioridazine significantly decreases the percentage of viable RLVMECs after 24 hours. **C**. Representative bright field images of RLVMEC morphology following thioridazine exposure. **p*<0.5, significantly different from DMSO. These data are representative of three separate experiments. Error bars are SEM.

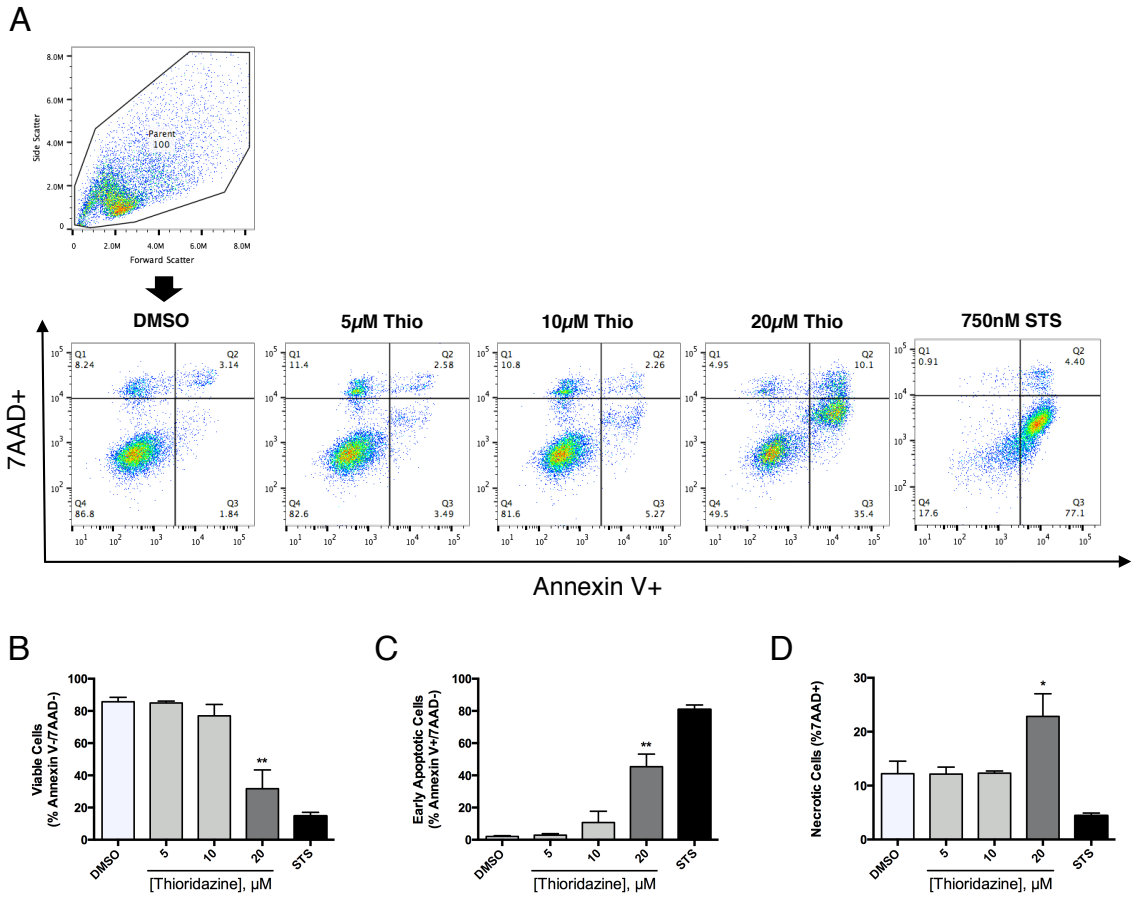

Figure 4. Thioridazine dose-dependently induces hallmarks of apoptosis and necrosis in RLMVECs after 24 hours. A. Representative flow cytometry scatter plots for RLVMECS co-stained with annexin V and 7AAD. **B.** 20 μM thioridazine significantly reduces the percentage of viable RLMVECs (Annexin V-/7AAD-) after 24 hours. **C.** 20 μM thioridazine significantly increases the percentage of early apoptotic RLVMECs (Annexin V+/7AAD-) after 24 hours. **D.** 20 μM thioridazine significantly increases the percentage of necrotic RLVMECs (7AAD+) after 24 hours. Staurosporine (STS) represents a positive control for apoptosis. *p<0.5, **p<0.01, significantly different from DMSO. These data are representative of three separate experiments. Error bars are SEM.

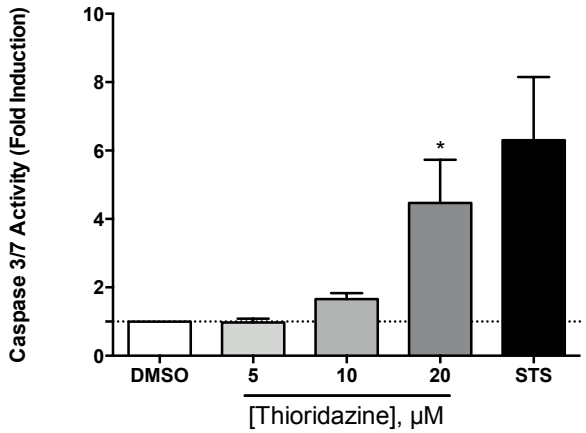

Figure 5. Thioridazine dose-dependently induces caspase 3/7 activity in RLMVECs after 24 hours. 20 µM thioridazine significantly induces caspase 3/7 activity in RLMVECs after 24 hours. Staurosporine (STS) represents a positive control for apoptosis. *p<0.5, significantly different from DMSO. These data are representative of three separate experiments. Error bars are SEM.

4.1.3 Thioridazine Down-regulates RLMVEC TCTP Levels

Compared to DMSO controls, RLMVECs treated with 10 μM thioridazine for 24 hours had significantly lower TCTP levels as determined by immunoblotting ($p<0.01$) (Figure 6).

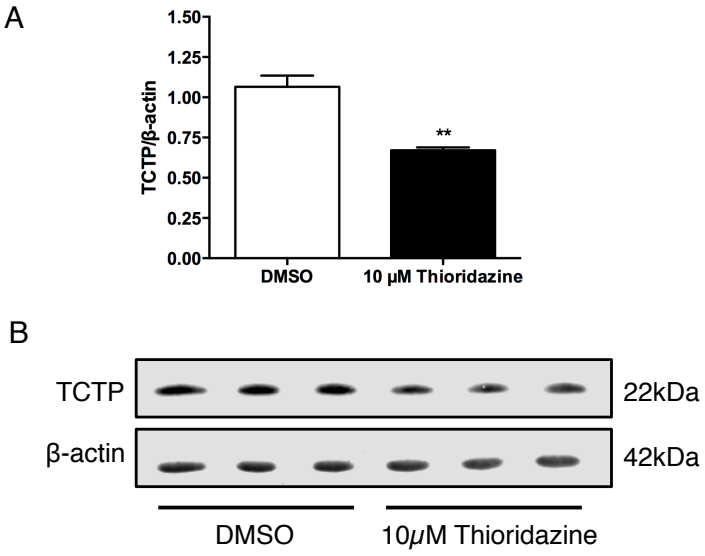

Figure 6. 10 μM thioridazine significantly down-regulates RLMVEC TCTP levels after 24 hours. A. Densitometry quantification of the immunoblot featured in panel B. **B.** TCTP immunoblot displaying three biological replicates. **p*<0.5, significantly different from DMSO. Error bars are SEM.

4.2 In Vivo

4.2.1 Pilot Study: Thioridazine & Sertraline in the SU/CH Rat Model

To examine the effects of thioridazine and sertraline in the SU/CH rat model of experimental PAH a pilot study was conducted in accordance with the experimental design described in section 3.2.1 (Figure 2).

4.2.1.1 Hemodynamics

Compared to vehicle controls, rats receiving 10 mg/kg/d thioridazine for three consecutive weeks showed no significant improvement in RVSP and no change in systemic arterial pressure (SAP) (Figures 7 & 8). However, this was largely due to the fact that one animal in the control group exhibited a surprising "spontaneous" improvement in RVSP that we have not seen previously in this model. When this animal was removed from the analysis (which was done only to inform whether further experiments might be warranted) the difference between endpoint measurements of RVSP for vehicle control and thioridazine treated rats was statistically significant ($p<0.01$). Furthermore, compared to controls, thioridazine appeared to limit the progression, and even modestly improve, RVSP. In contrast to previous findings in the MCT rat model of experimental PH (Li et al., 2006), the administration of 10 mg/kg/d sertraline for three consecutive weeks had no significant effects on RVSP in the SU/CH rat model of PAH (Figures 7 & 8).

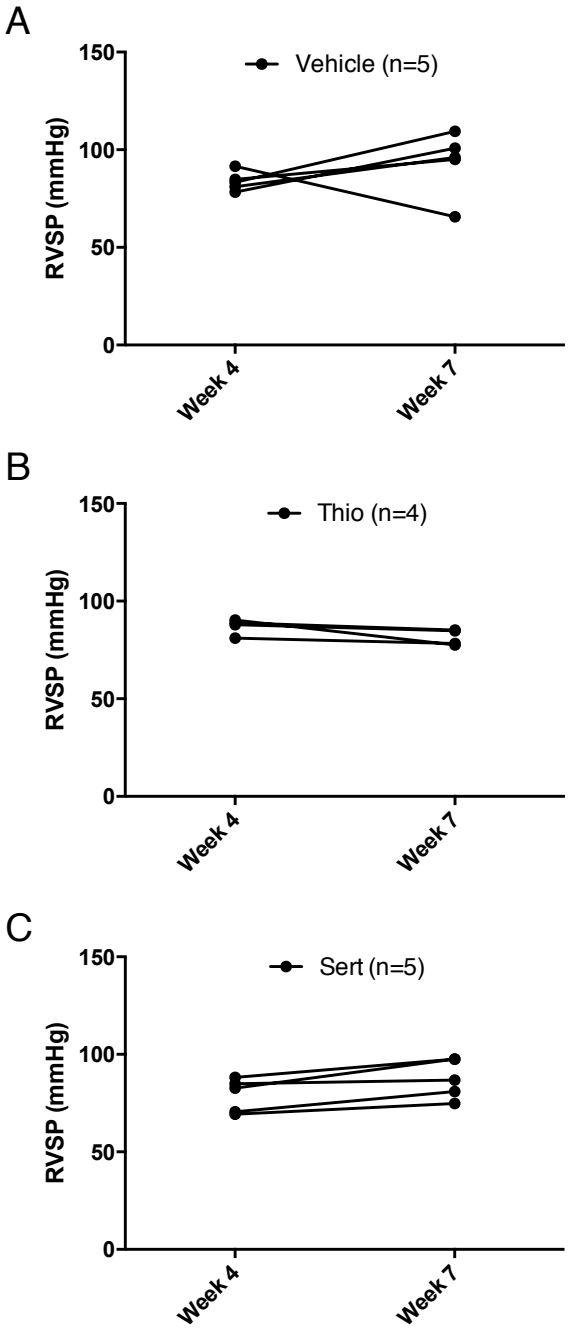

Figure 7. Baseline and endpoint measurements of RVSP from SU/CH rats treated with thioridazine, sertraline, or vehicle. A. Individual animal data for rats receiving vehicle control. Note the single rat showing spontaneous improvement in RVSP. **B.** Individual animal data for rats receiving thioridazine. **C.** Individual animal data for rats receiving sertraline. RVSP, right ventricular systolic pressure.

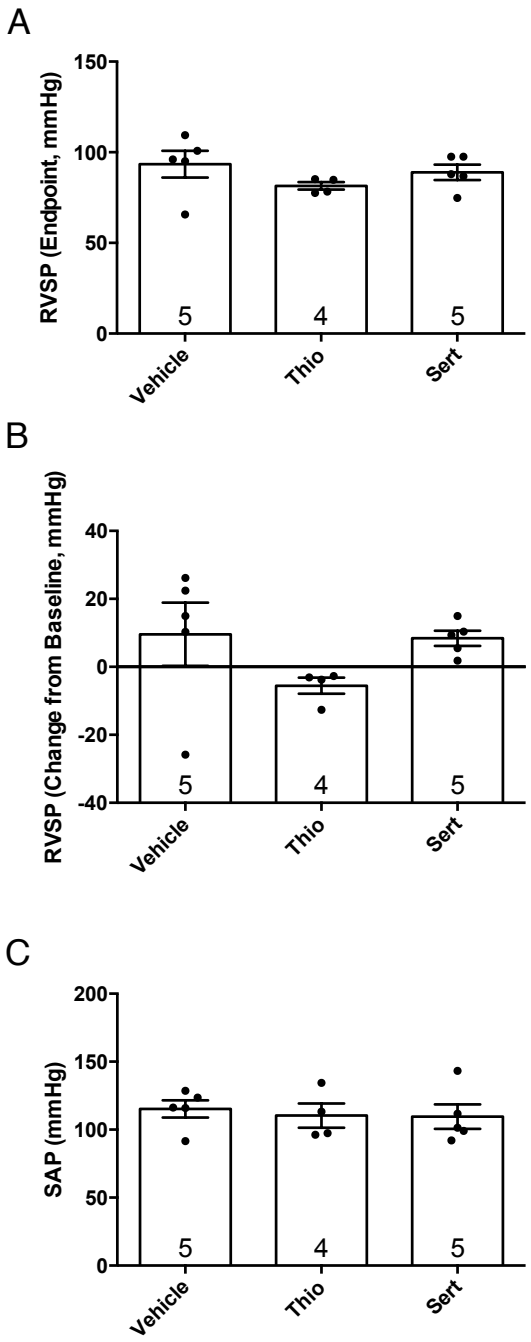

Figure 8. Endpoint measurements of RVSP and SAP from SU/CH rats treated with thioridazine, sertraline, or vehicle. A. RVSP at endpoint. **B.** Absolute change in RVSP from week 4 baseline to week 7 endpoint **C.** SAP at endpoint. RVSP, right ventricular systolic pressure; SAP, systemic arterial pressure. Error bars are SEM.

4.2.1.2 Cardiac Function & Structure

SU/CH rats treated with thioridazine or sertraline showed no significant differences in PAAT, CO, SV, or HR compared to controls (Figures 9 & 10). However, direct measurements of right ventricle mass suggested that thioridazine may have modestly inhibited the progression of RVH (Figure 11A). In support of this finding, echocardiographic analyses showed that thioridazine treated rats tended to have smaller RVID and lower RVID/LVID ratios compared to controls, although these measurements were not statistically significant (Figures 11C, 11D & 12). In contrast to these findings, thioridazine treated rats displayed a significant decrease in TAPSE compared to controls, which is indicative of worsened right ventricle function ($p<0.01$) (Figure 11E).

4.2.1.3 TCTP Lung Immunoblotting & Immunohistochemistry

Whole lung homogenate immunoblotting and immunohistochemical staining for TCTP revealed no significant differences between thioridazine and vehicle control treated SU/CH rats (Figures 13 & 14). Similarly, whole lung homogenate immunoblotting and immunohistochemical staining for TCTP revealed no significant differences between sertraline and vehicle control treated SU/CH rats (Figure 15 & 16).

4.2.1.4 Vessel Obliteration & Adventitial Cell Clearance

Periadventitial inflammation was visually assessed in the pulmonary vessels (<150μm) of SU/CH rats receiving thioridazine, sertraline, or vehicle. As expected, control rats displayed a consistent accumulation of mononuclear cells around remodelled arteries. Interestingly, in thioridazine treated rats, this was less consistent and often the

periadventitial zone appeared devoid of cells, consistent with the clearance of cells. However, quantitative assessment of adventitial "clear zones" revealed no significant differences between groups (Figure 17). A t-test analysis with a post-hoc Sidak-Bonferroni to correct for multiple comparisons found no significant differences between the degrees of vessel obliteration between groups (Figure 18).

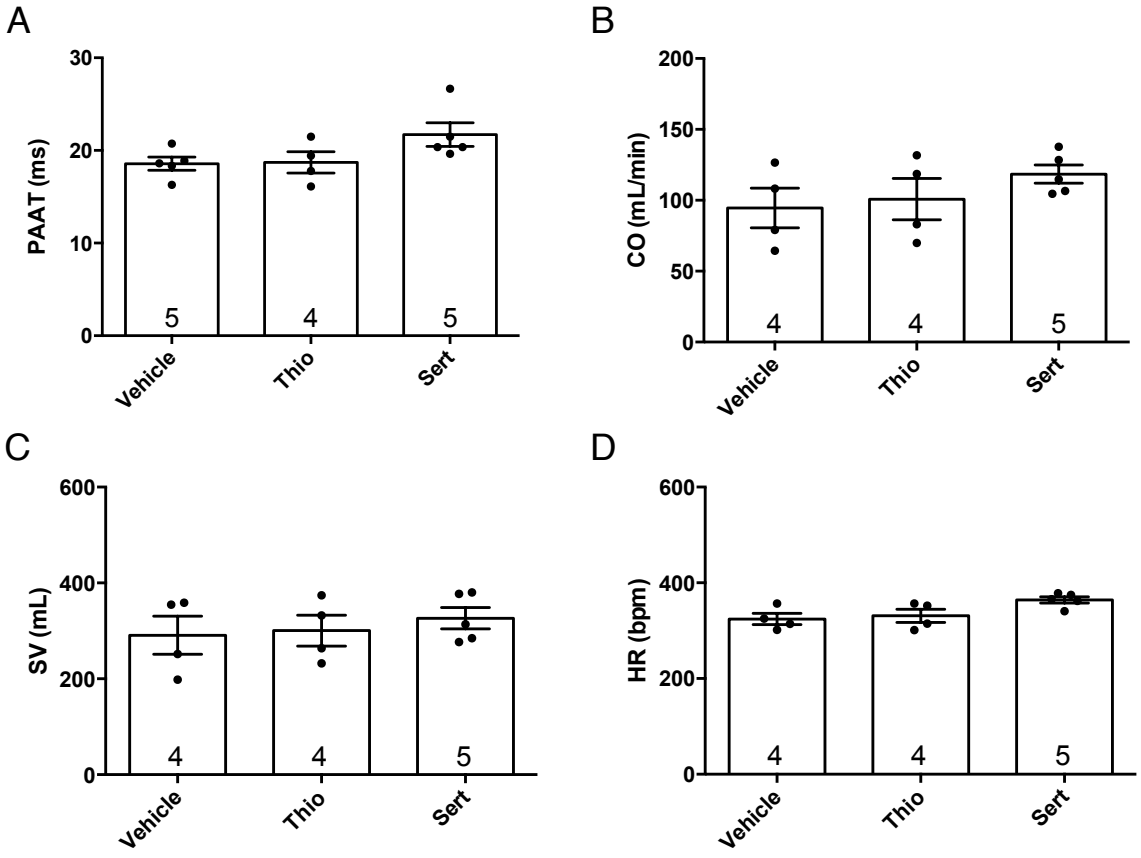

Figure 9. Endpoint measurements of cardiac function from SU/CH rats treated with thioridazine, sertraline, or vehicle. A - D. Compared to vehicle control, neither thioridazine nor sertraline had any significant effects on PAAT, CO, SV, or HR. PAAT, pulmonary arterial acceleration time; CO, cardiac output; SV, stroke volume; HR, heart rate. Error bars are SEM.

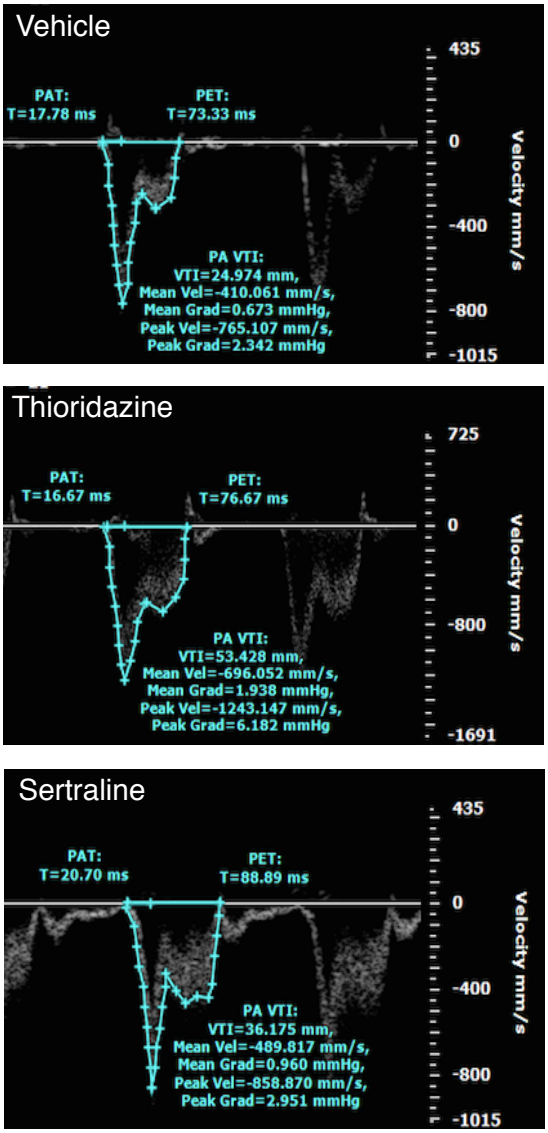

Figure 10. Representative endpoint pulse-wave Doppler images of pulmonary arterial blood flow from SU/CH rats treated with thioridazine, sertraline, or vehicle. PAT, pulmonary acceleration time; PET, pulmonary ejection time; PA VTI, pulmonary arterial velocity time integral; Vel, velocity; Grad, gradient.

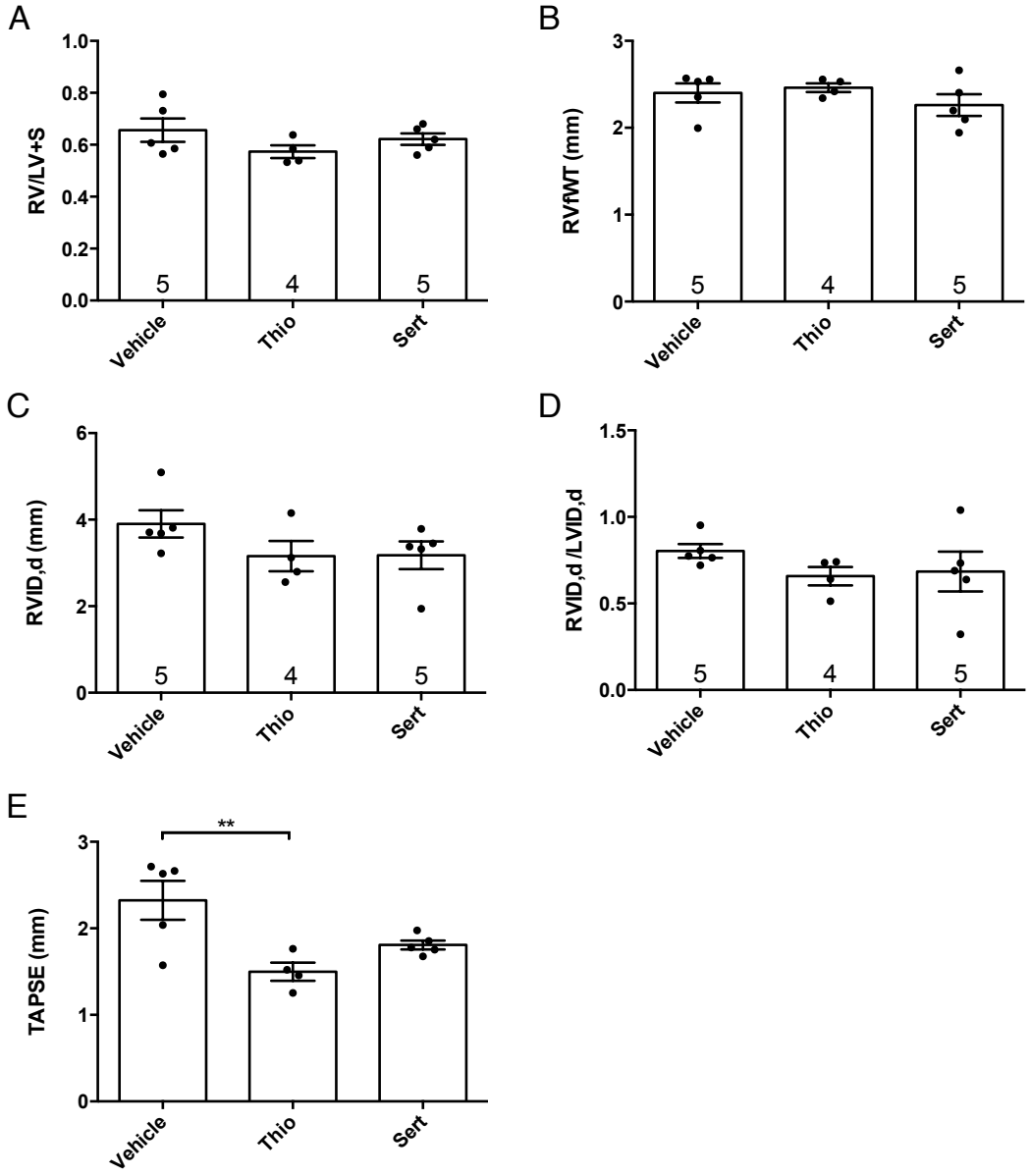

Figure 11. Endpoint measurements of right ventricular structure and function from SU/CH rats treated with thioridazine, sertraline, or vehicle. A. Right ventricular hypertrophy index (RV/LV+S). **B.** RVfWT at end diastole. **C.** RVID at end diastole. **D**. RVID/LVID ratio at end diastole. **E.** Compared to controls, rats receiving thioridazine displayed a significant decrease in TAPSE. RV, right ventricle; LV, left ventricle, S, septum; RVfWT, right ventricle free wall thickness, RVID,d, right ventricle internal diameter at end diastole; LVID,d, left ventricle internal diameter at end diastole; TASPE, tricuspid annular plane systolic excursion. ** $p<0.01$, significantly different from DMSO. Error bars are SEM.

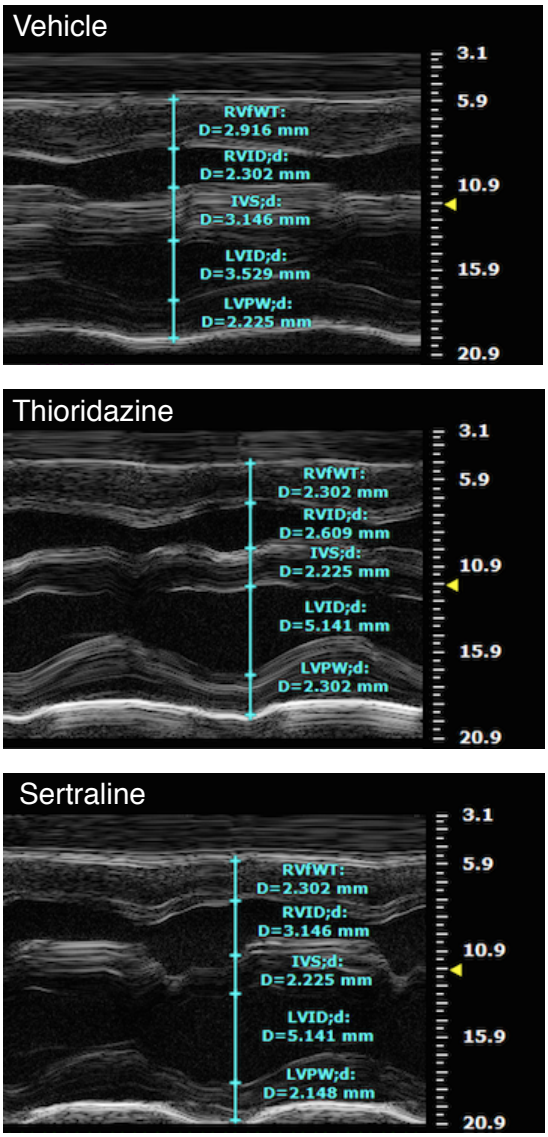

Figure 12. Representative endpoint M-mode parasternal short-axis views of the right and left ventricles from SU/CH rats treated with thiordiazine, sertraline, or vehicle. RVfWT, right ventricle free wall thickness; RVID,d, right ventricle internal diameter at end diastole; IVS,d, interventricular septum at end diastole; LVID,d, left ventricle internal diameter at end diastole; LVPW,d, left ventricular posterior wall thickness at end diastole.

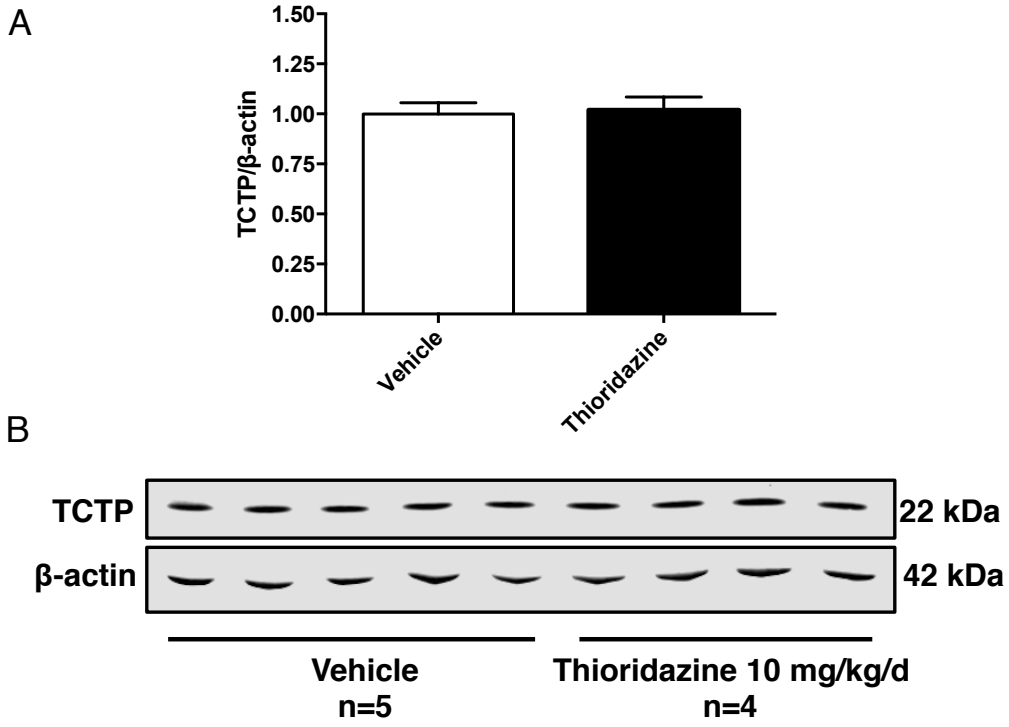

Figure 13. Thioridazine does not down-regulate TCTP levels in whole lung homogenates from SU/CH rats. A. Densitometry quantification of immunoblot featured in panel B. **B.** TCTP immunoblot displaying biological replicates from SU/CH rats treated with vehicle control and thioridazine (n=5 and n=4, respectively). Error bars are SEM.

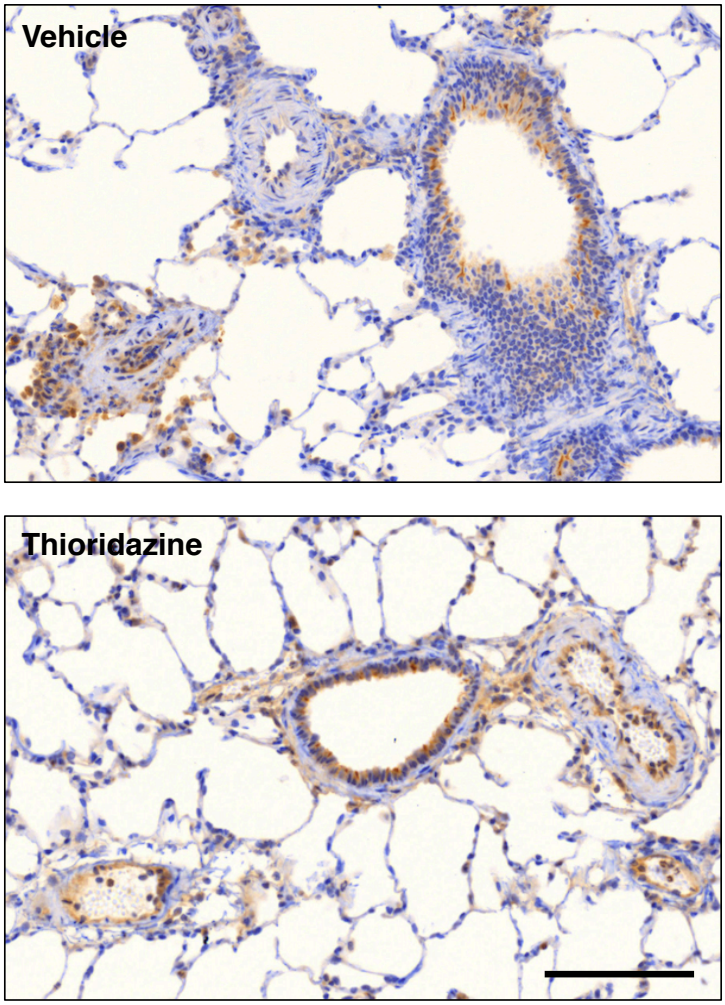

Figure 14. Representative images of lung TCTP immunohistochemistry from SU/CH rats treated with thioridazine or vehicle. Vehicle control (top) and thioridazine treated (bottom). Scale bar = 100μm.

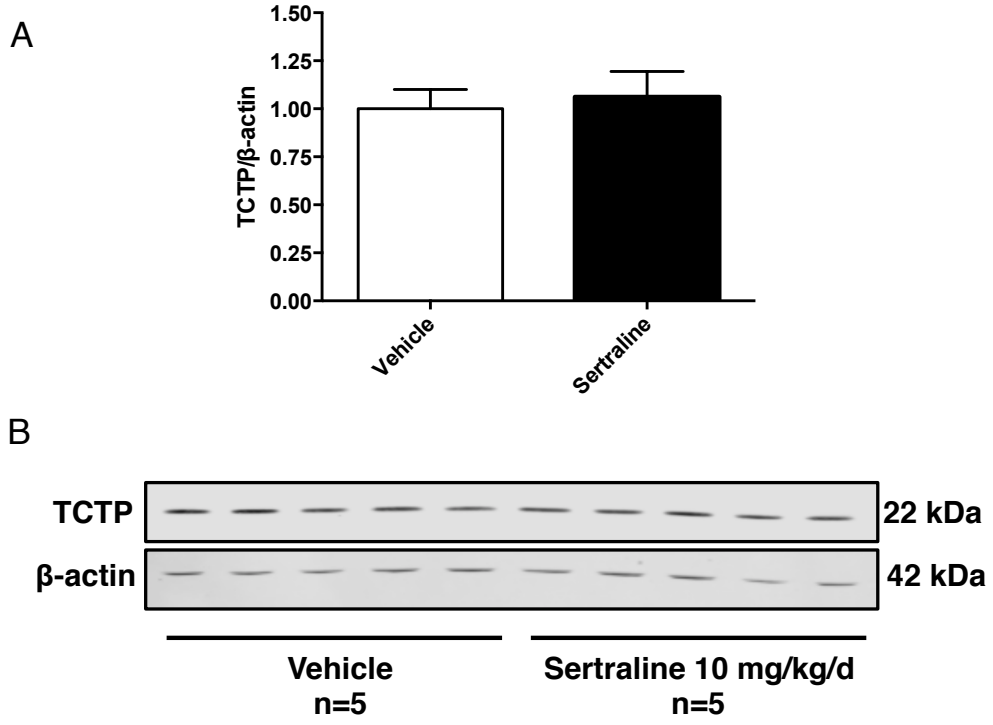

Figure 15. Sertraline does not down-regulate TCTP levels in whole lung homogenates from SU/CH rats. A. Densitometry quantification of immunoblot featured in panel B**. B.** Immunoblot displaying biological replicates from SU/CH rats treated with vehicle control and sertraline (n=5 and n=5, respectively). Error bars are SEM.

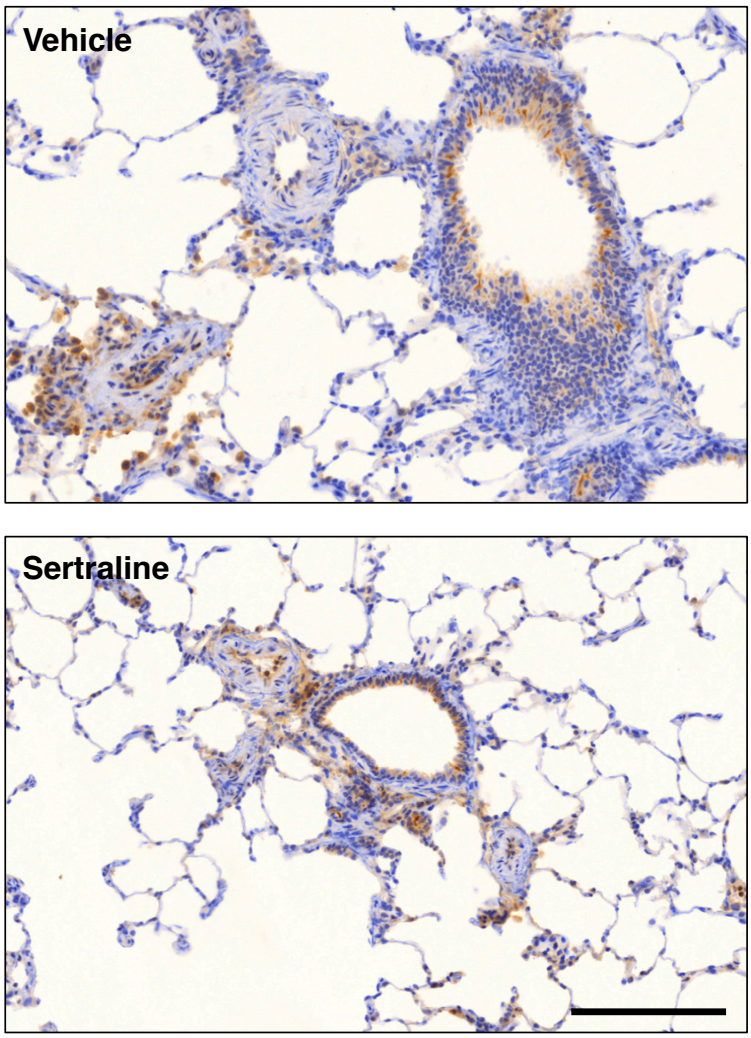

Figure 16. Representative images of lung TCTP immunohistochemistry from SU/CH rats treated with sertraline or vehicle. Vehicle control (top) and sertraline treated (bottom). Scale bar = 100μm.

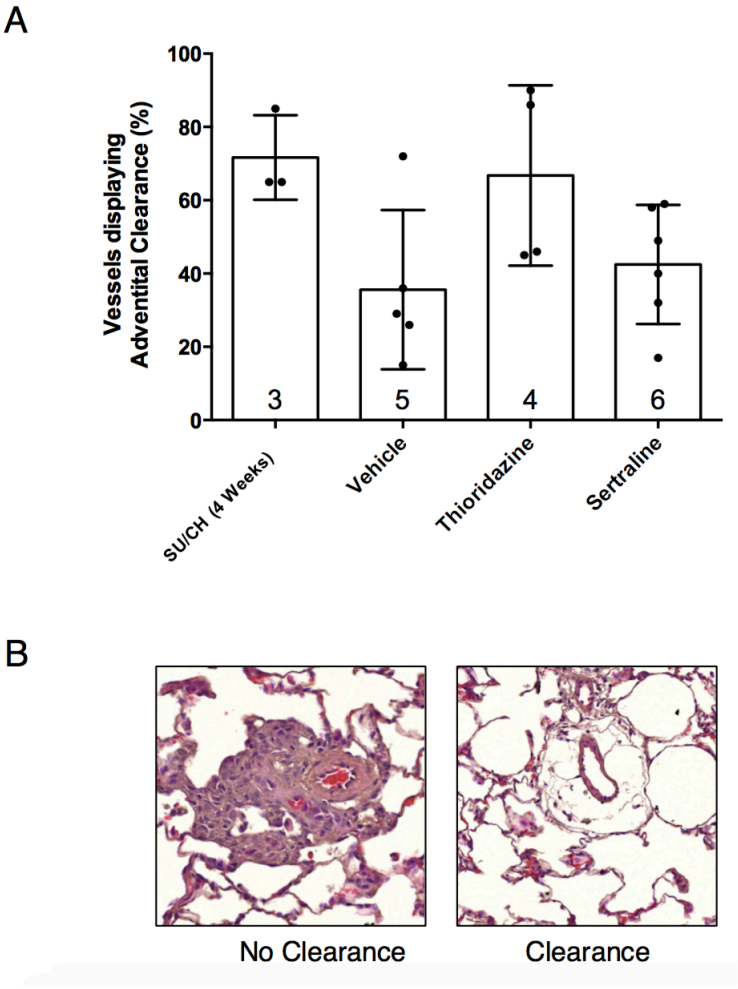

Figure 17. Endpoint quantification of adventitial cell clearance from SU/CH rats treated with thioridazine, sertraline, or vehicle. A. Compared to SU/CH rats receiving vehicle control, the pulmonary vessels of rats receiving thioridazine or sertraline showed no significant differences in adventitial cell clearance at the experimental endpoint. **B.** Examples of a pulmonary vessels displaying no adventitial cell clearance (left) and almost complete clearance (right). Error bars are SEM.

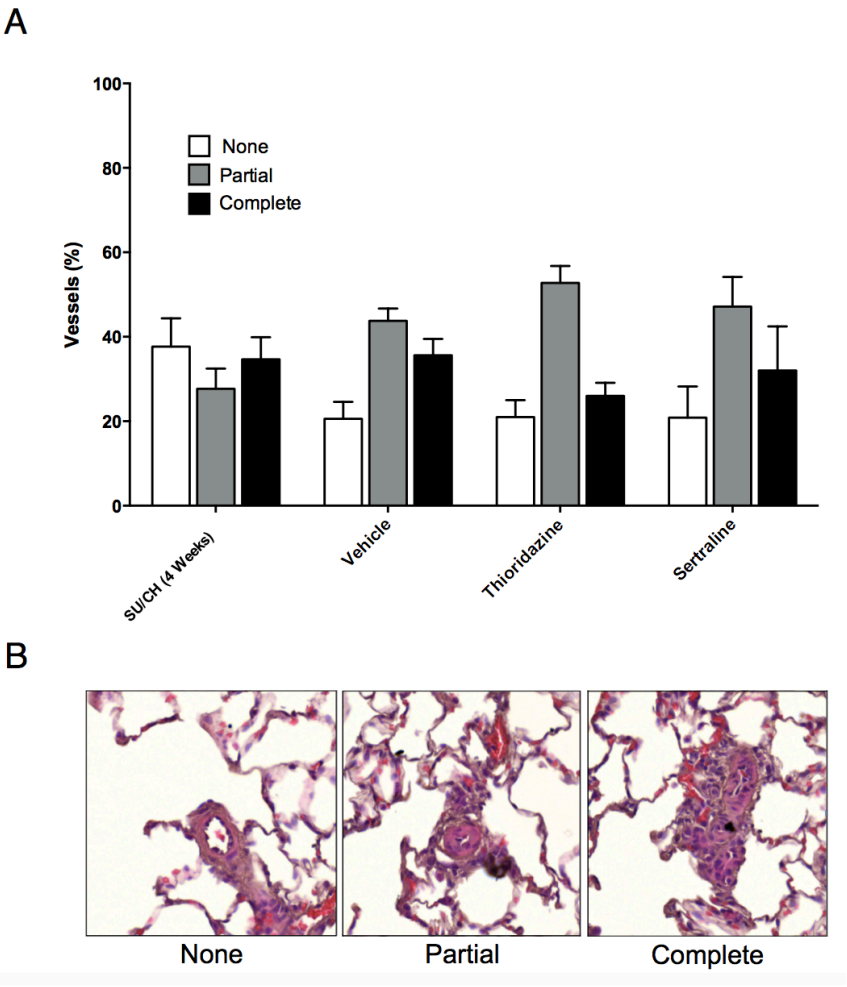

Figure 18. Endpoint quantification of pulmonary vessel obliteration from SU/CH rats treated with thioridazine, sertraline, or vehicle. A. Vessel obliteration scoring prior to treatment (i.e. SU/CH at the end of week 4) (n=3), following the delivery of vehicle (n=5), following the delivery of thioridazine (n=4), and following the delivery of sertraline (n=6). **B.** Examples of varying degrees of vessel obliteration. Error bars are SEM.

4.2.2 Second Study: Validation of Thioridazine in the SU/CH Rat Model

Given the inconclusive results of the pilot study, a second study with a greater number of rats was performed using the same dose of thioridazine. While 10 mg/kg/d thioridazine did not appear to down-regulate lung TCTP levels in the pilot study, this dose appeared to be having a positive effect on relevant physiological parameters and was tolerated well by the animals. Also, thioridazine may well inhibit the interaction of TCTP with its multiple partners without an overall reduction in TCTP levels (Amson et al., 2012). In order to maximize statistical power, the results presented below are a combination of both the pilot study data and the results of the follow-up study.

4.2.2.1 Hemodynamics, Cardiac Function & Cardiac Structure

In a contrast to the results of the pilot study, thioridazine had no discernable effects on any of the hemodynamic or cardiac parameters evaluated when these data were combined in the larger follow up study (Figures 19, 20, & 21).

4.2.2.2 Vessel Obliteration & Adventitial Cell Clearance

Similarly, there was no evidence to suggest that thioridazine had any significant effect of pulmonary vascular obliteration or adventitial cell clearance when the data from the two studies were combined (Figures 22 & 23).

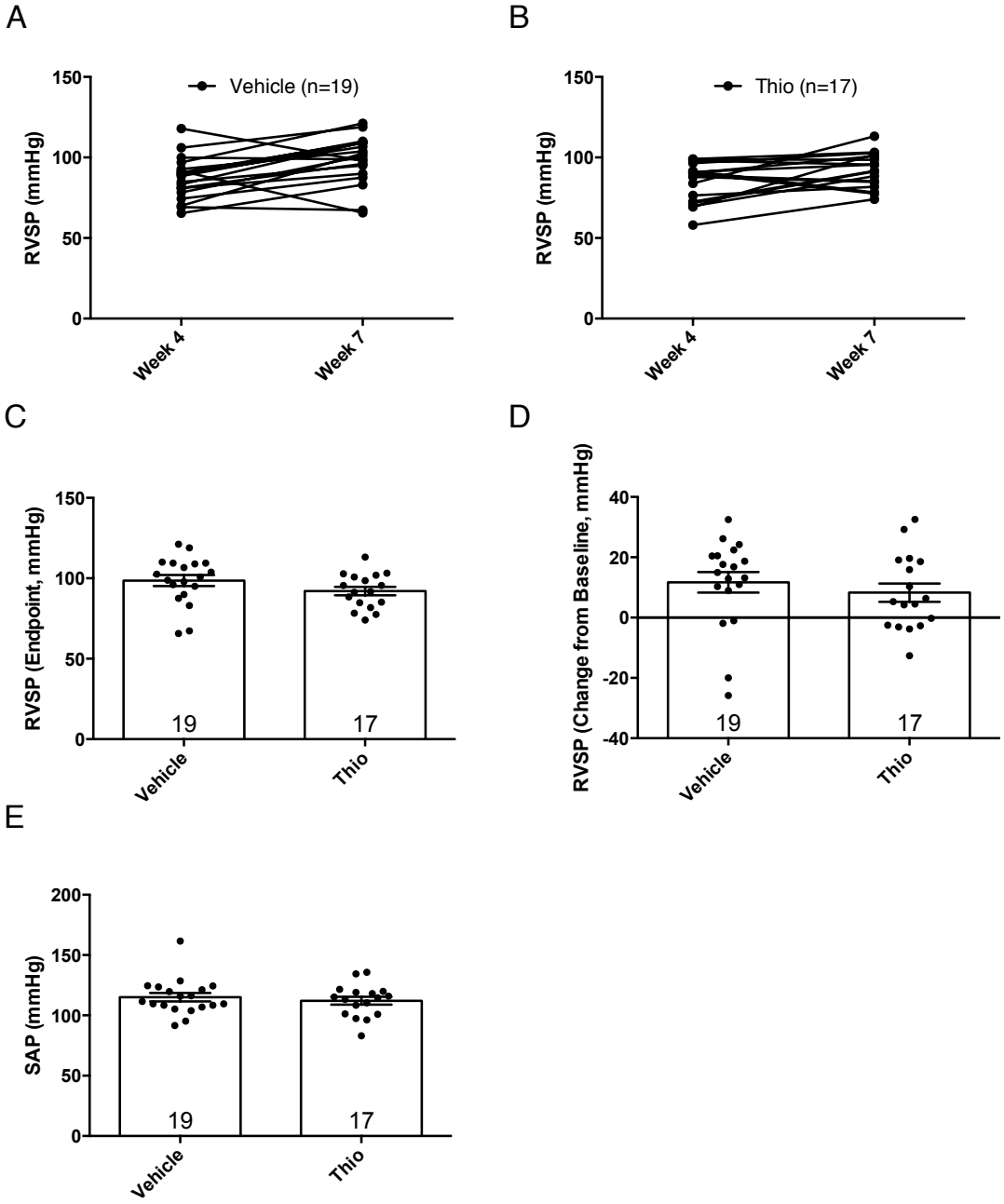

Figure 19. Thioridazine has no effect on RVSP or SAP in the SU/CH rat model. **A**. Individual animal data for SU/CH rats receiving vehicle control between week 4 and 7. **B.** Individual animal data for SU/CH rats receiving thioridazine between week 4 and 7. **C.** RVSP at endpoint. **D.** Absolute change in RVSP from week 4 baseline to week 7 endpoint. **E.** SAP at week 7 endpoint. RVSP, right ventricular systolic pressure; SAP, systemic arterial pressure. Error bars are SEM. The results displayed include data from vehicle and thioridazine treated SU/CH rats collected during the pilot study.

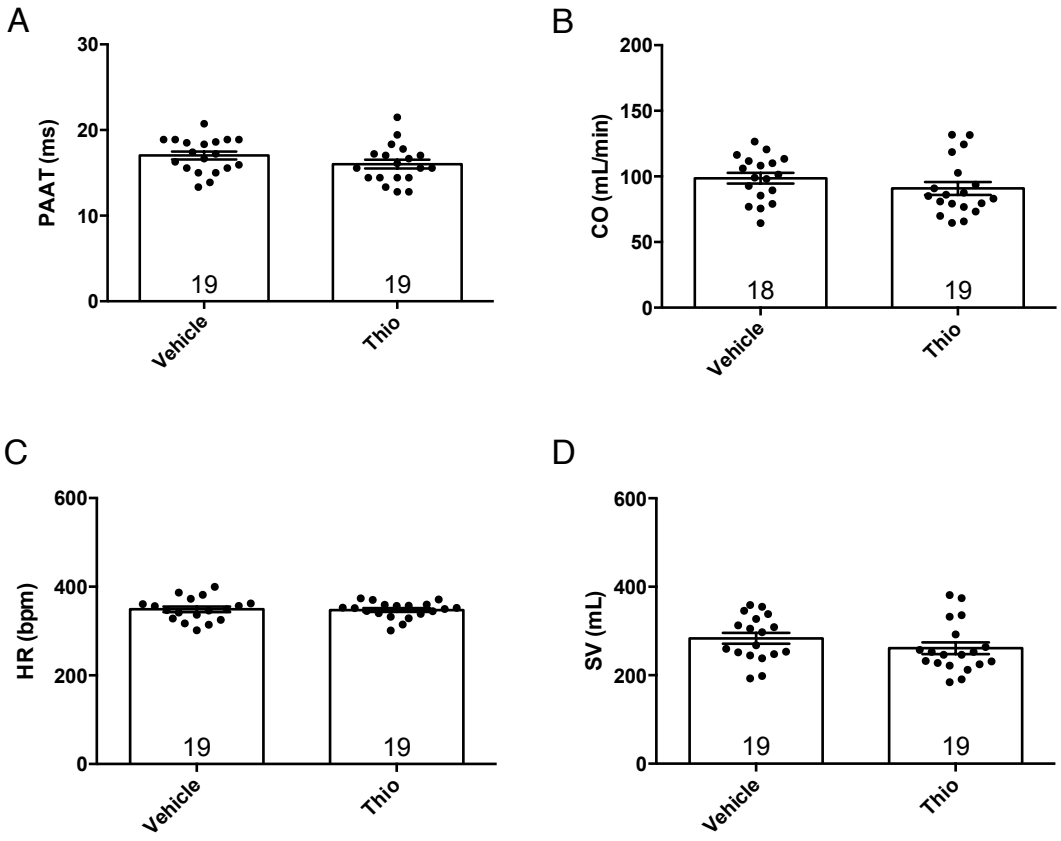

Figure 20. Thioridazine has no effect on endpoint measurements of cardiac function in the SU/CH rat model. A - D. Compared to vehicle control, thioridazine had no significant effects on PAAT, CO, SV, or HR. PAAT, pulmonary arterial acceleration time; CO, cardiac output; SV, stroke volume; HR, heart rate. Error bars are SEM. The results displayed include data from vehicle and thioridazine treated SU/CH rats collected during the pilot study.

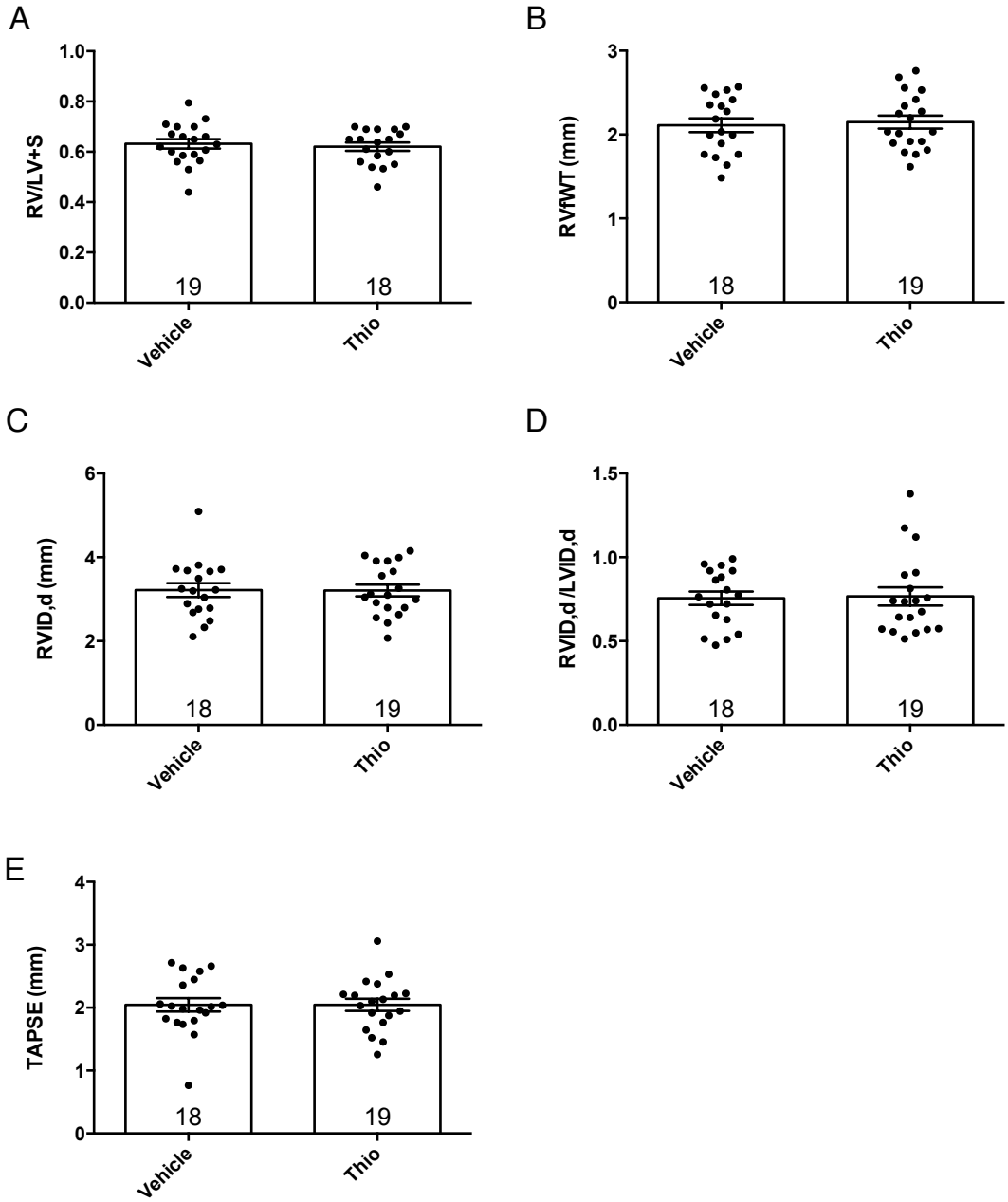

Figure 21. Thioridazine has no effect on endpoint measurements of right ventricular structure or function in the SU/CH rat model. Right ventricular hypertrophy index (RV/LV+S). **B.** RVfWT at end diastole. **C.** RVID at end diastole. **D**. RVID/LVID ratio at end diastole. **E.** TAPSE. RV, right ventricle; LV, left ventricle, S, septum; RVfWT, right ventricle free wall thickness, RVID,d, right ventricle internal diameter at end diastole; LVID,d, left ventricle internal diameter at end diastole; TASPE, tricuspid annular plane systolic excursion. Error bars are SEM. The results displayed include data from vehicle and thioridazine treated SU/CH rats collected during the pilot study.

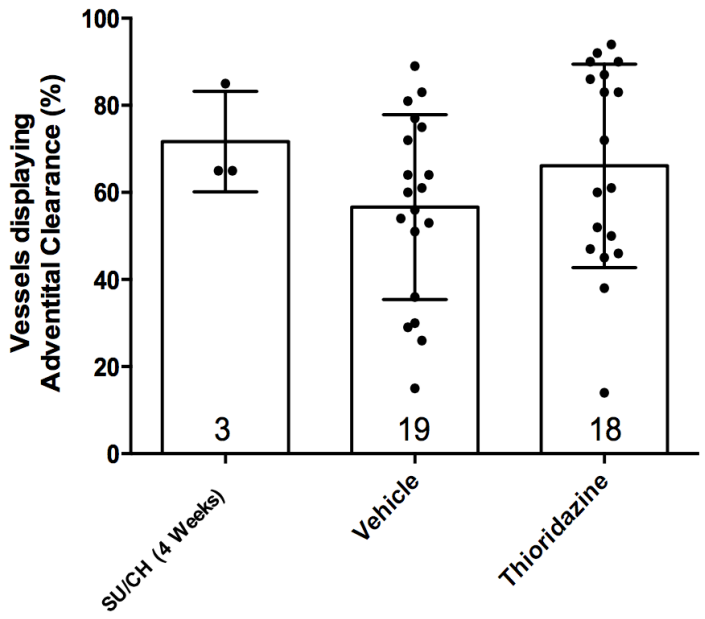

Figure 22. Thioridazine has no effect on adventitial cell clearance in the SU/CH rat model. Compared to SU/CH rats receiving vehicle control, the pulmonary vessels of rats receiving thioridazine showed no evidence of improved adventitial cell clearance at the experimental endpoint. Error bars are SEM. The results displayed include data from vehicle and thioridazine treated SU/CH rats collected during the pilot study.

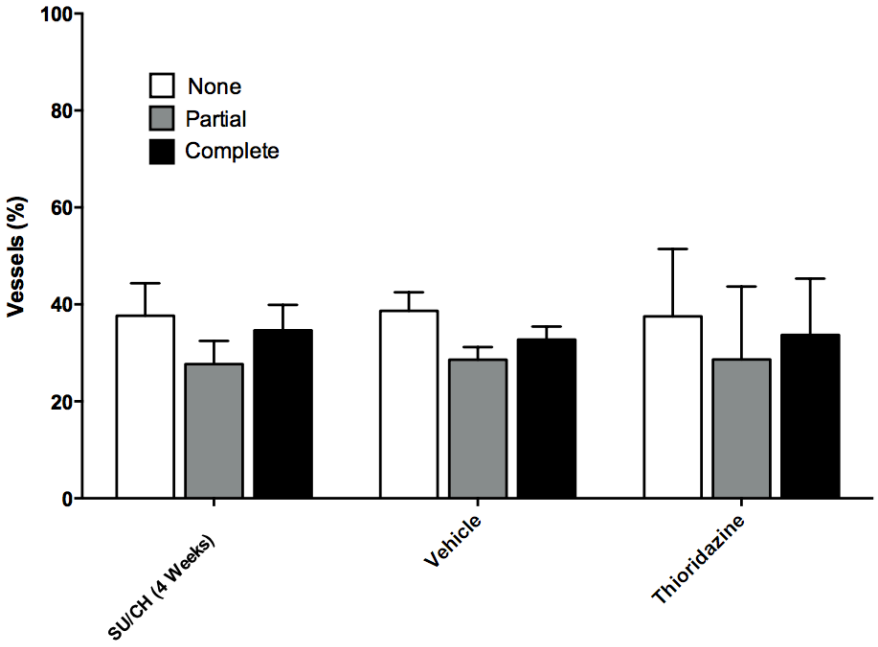

Figure 23. Thioridazine has no effect on pulmonary vessel obliteration in the SU/CH rat model. Vessel obliteration scoring prior to treatment (i.e. SU/CH at the end of week 4) (n=3), following the delivery of vehicle (n=19), and following the delivery of thioridazine (n=18). Error bars are SEM. The results displayed include data from vehicle and thioridazine treated SU/CH rats collected during the pilot study.

4.2.3 TCTP & CD68 Immunofluorescence in the SU/CH Rat Model

Immunofluorescence staining for TCTP and α-smooth muscle actin in serial lungs sections from untreated SU/CH rats at the experimental endpoint show minimal signal overlap (Figure 24). TCTP probe fluorescence appeared most predominantly in pulmonary adventitia and the vessel lumen (Figure 24). As previously reported in rats injected with SU5416 only (Lavoie et al., 2014), TCTP and monocyte/macrophage marker CD68 immunofluorescence was detectable in corresponding areas of the adventitia (Figure 24). This finding provided further evidence to support a connection between TCTP expression and inflammation in complex vascular lesions.

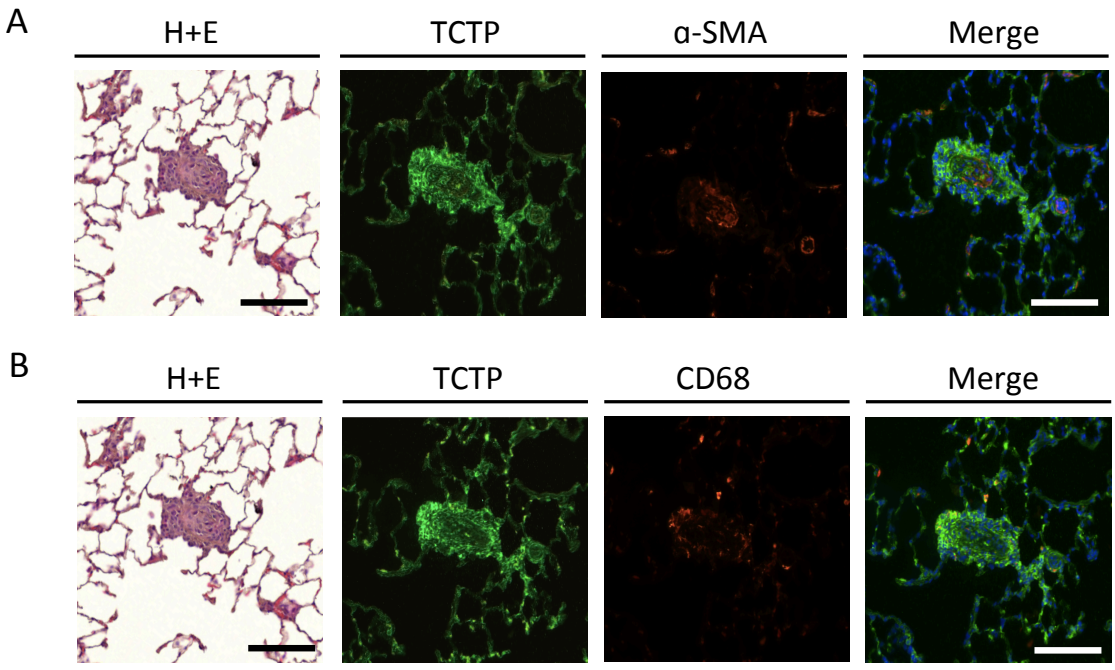

Figure 24. Representative H+E and immunofluorescence staining for TCTP, CD68, and α-SMA in the SU/CH rat model. A. Serial lung sections stained with H+E, TCTP, and α-SMA. TCTP immunofluorescence appeared predominantly in the adventitial layer and intimal layer of remodeled vessels in SU/CH rats, but did not appear to overlap with α-SMA staining. **B.** Serial lung sections stained with H+E, TCTP, and monocyte/macrophage marker CD68. Both TCTP and CD68 immunofluorescence was detected proximal to the adventitia. Scale bar = 100μm.

DISCUSSION

5.1 General Discussion

TCTP represents a potential new target for novel therapeutic interventions in PAH. As described in our 2014 Circulation report, TCTP was identified following a high-throughput screen comparing the proteomic profiles of BOECs from HPAH patients with identified *Bmpr2* mutations to BOECs from healthy age-matched controls (Lavoie et al., 2014). Although the screening revealed several significantly up-regulated and down-regulated proteins in PAH BOECs, TCTP was selected for further study based on previous reports implicating the protein in processes such as malignant transformation, chronic non-resolving inflammation, and vascular cell survival. We hypothesized that TCTP was involved in a molecular nexus linking *Bmpr2* mutations to pulmonary EC apoptosis and the emergence of growth-dysregulated vascular cells. Specifically, we hypothesized that increased TCTP expression contributed to the emergence of growth-dysregulated, apoptosis-resistance ECs associated with vascular remodelling and that targeting TCTP with known small molecule inhibitors could prevent or reverse vascular remodelling in the SU/CH rat model of PAH.

In vitro, the effects of 24 hour thioridazine exposure on RLMVEC viability and TCTP protein levels were examined. Our results demonstrate that thioridazine dose-dependently decreases RLMVEC viability, significantly reduces TCTP abundance, and induces a partially apoptotic phenotype in RLMVECs. These findings are consistent with previous reports demonstrating the ability of thioridazine to induce apoptosis and down-regulate TCTP in tumour cells (Amson et al., 2012; Tuynder et al., 2004).

In vivo, we attempted to down-regulate TCTP in the pulmonary vasculature of

SU/CH rats using two previously identified TCTP small molecule inhibitors, thioridazine and sertraline. Unfortunately, despite promising preliminary results, neither small molecule had beneficial effects on hemodynamic, echocardiographic, or histological parameters. In regards to inflammation, immunofluorescence staining revealed that TCTP and CD68-positive cells appeared to co-localize in the adventitial layer of remodelled vessels. This result confirms our previous observations in the SU5416 rat model and further highlights the potential inflammatory role of TCTP in PAH.

5.2 Potential Reasons for the Lack of In Vivo Efficacy with TCTP Inhibitors

Much like human PAH, vascular remodelling in the SU/CH rat model is progressive (Abe et al., 2010; Toba et al., 2014). Evidence suggests that EC apoptosis is an essential trigger for the initiation of human PAH, and indeed, the SU/CH model is induced by inhibition of VEGFR2 leading to widespread EC apoptosis in the lung microvasculature (Taraseviciene-Stewart et al., 2001). As the disease progresses, it is believed that EC apoptosis gives way to the emergence of hyperproliferative, apoptosis-resistant ECs which are involved in vascular remodelling (Jurasz et al., 2010). Thus, TCTP inhibition at later stages of the SU/CH model would be expected to be beneficial by reducing the survival of these quasi-neoplastic vascular cells, whereas inhibition of TCTP early on could exacerbate, rather than prevent, PAH by further increasing the susceptibility of lung vascular ECs to apoptosis.

In order to target growth-dysregulated ECs in the SU/CH model, we waited until four weeks had elapsed before administering our TCTP small molecule inhibitors. As evidenced by our histological analyses, this is a time point at which substantial vascular

remodelling has already occurred in this model. However, since designing these *in vivo* experiments our lab has observed that apoptosis and growth-dysregulation of ECs may coexist in the SU/CH model beyond three weeks (Ketul Chaudhary, unpublished data), a much later time point than previously known. To some extent, the fact that both increased apoptosis and EC growth-dysregulation coexists this late in the model may help explain our inconsistent and largely negative *in vivo* results. While thioridazine may have had positive therapeutic effects on growth-dysregulated pulmonary ECs, it may have also had detrimental effects by exacerbating apoptosis or necrosis. In comparison to our recent observations in the SU/CH mode, it is unknown whether or not EC apoptosis and growth-dysregulation are temporally segregated or occur simultaneously in human PAH. The exact timing of these processes will likely remain unknown until the progression of PAH can be assessed using non-invasive techniques, such as nuclear imaging of annexin V (Paffett et al., 2012), or it becomes feasible to obtain lung specimens that are representative of the earlier stages of this disease.

While neither thioridazine nor sertraline demonstrated the ability to down-regulate lung TCTP levels in SU/CH rats, it is possible that these small molecules may inhibit the activity of TCTP without detectable changes in protein abundance. For example, Amson and colleagues have shown that both thioridazine and sertraline are able to directly bind and inhibit TCTP *in vitro* (Amson et al., 2012). In the same study, the authors also reported that both thioridazine and sertraline inhibit the co-immunoprecipation of TCTP and MDM2, a well-known TCTP binding partner (Amson et al., 2012). These findings suggest that thioridazine and sertraline may inhibit TCTP by preventing the protein's ability to bind to other partners rather than by simply decreasing

abundance. To the best of our knowledge, the mechanisms by which thioridazine and sertraline may down-regulate or inhibit TCTP *in vivo* are still unknown. Thus, future studies are warranted to fully examine the *in vivo* effects of thioridazine and sertraline on TCTP activity, expression, and signalling in the pulmonary vasculature.

There are several other additional plausible explanations as to why both thioridazine and sertraline failed to detectably down-regulate TCTP in the lungs of SU/CH rats. The most readily apparent explanation is that the chosen dose of 10 mg/kg/d was inadequate to achieve the desired effect. Prior to beginning our *in vivo* experiments we considered performing preliminary dose-ranging studies to determine the required dose to down-regulate TCTP in the lungs of SU/CH rats. However, we decided to forego these studies given the fact that sertraline delivered at 10 mg/kg/d had been previously effective in the MCT rat model and that 10 mg/kg/d is broadly considered to be physiologically relevant dose of thioridazine in rats (Haduch et al., 2007; Maj et al., 1979; Shi et al., 2012; Wojcikowski & Daniel, 2002). Our preliminary pilot studies led us to believe that thioridazine delivered at 10 mg/kg/d was sufficient to induce a modest therapeutic effect and so we proceeded to validate our pilot results with a larger cohort of animals. Despite our promising preliminary results, the trend we initially observed did not hold. While it is unclear why we observed a discrepancy between our initial pilot study and our follow-up study, it is likely that the trend observed in the initial study could have been due to mere chance alone given the limited number of animals.

5.3 Other Considerations & Limitations

Small molecules have the inherit disadvantage of being non-specific; that is to say, small molecules can have a number of off-target effects when delivered *in vivo*. It is well known that both thioridazine and sertraline interact with a variety of biological targets, such as SERT and various dopamine receptors. Thus, in the event that either thioridazine or sertraline contributed to a significant improvement in SU/CH rats, such findings would have had to be interpreted in light of the potential influence of off-target effects. Naturally, such a scenario was considered prior to the start of experimentation; however, given the fact that both sertraline and thioridazine had been previously approved for human use, it was attractive to prioritize evaluating their efficacy in the SU/CH model in hopes of clinical translation despite consciously conceding some aspects of internal validity.

A major limitation of the *in vitro* experiments presented in this thesis is that they focus exclusively on the effects of thioridazine on RLMVEC death, necrosis, and TCTP abundance. Additional assays evaluating other relevant EC functions, such angiogenesis, migration, invasion, or proliferation, could have broadened our current understanding of the effects of thioridazine on ECs *in vitro*. Studies utilizing human umbilical cord ECs have demonstrated the ability of thioridazine to inhibit VEGF-stimulated proliferation, invasion, migration, and capillary-like tube formation (Byun et al., 2012). As well, thioridazine has been shown to significantly decrease the growth and vascularity of human ovarian tumour xenographs implanted in nude mice (Park et al., 2014). When compared to tumours from control mice, tumours from mice treated with thioridazine displayed increased expression of the pro-apoptotic markers p53 and Bax, and decreased

expression of the anti-apoptotic markers Bcl-2 and survivin (Park et al., 2014). The ability of thioridazine to inhibit angiogenesis creates a potential challenge for adopting this small molecule as a therapy for PAH. For example, it may be difficult to balance thioridazine's pro-apoptotic effects on growth-dysregulated, highly proliferative ECs with its reported ability to inhibit angiogenesis, which may be beneficial in PAH by regenerating lost or damaged microvasculature.

Another limitation of our *in vitro* experiments is that only one cell type was utilized. The information that we collected from our experiments could have been more informative if we incorporated studies of human pulmonary artery EC or BOECs. Such experiments may have involved comparative analyses of the effects of TCTP small molecule inhibitors on BOECs with abundant TCTP expression from HPAH patients and BOECs with normal TCTP expression from healthy individuals. Moreover, a TCTP overexpressing cell line would have served as a useful tool for examining the molecular mechanisms underlying thioridazine-mediated apoptosis. Unfortunately, our attempts to develop TCTP overexpressing RLMVECs were unsuccessful.

5.4 Relevance to Human PAH

Sertraline is best known for its ability to selectively inhibit the reuptake of serotonin by blocking the activity of SERT. While SERT is most often associated with the termini of neurons, where it facilitates the uptake of serotonin following its release into the synaptic cleft, SERT can also be found on the cell membranes of pulmonary artery smooth muscle cells and fibroblasts (Thomas et al., 2013). Along with serotonin receptors, SERT plays an important role in mediating paracrine serotonin signalling

between pulmonary smooth muscle cells and pulmonary ECs (Thomas et al., 2013). Pulmonary ECs synthesize and release serotonin which induces pulmonary artery smooth muscle cell vasoconstriction and proliferation (Thomas et al., 2013).

Both clinical and pre-clinical studies have highlighted the potential role of serotonin and SERT in PAH pathology. Serotonin was first implicated in the pathogenesis of PAH in the 1960s, and again the 1980s, following an increase of "primary" PH cases associated with use of anorexigens such as aminorex and dexfenfluramine (MacLean, 2007). Although the exact explanation as to why these anorexigens increased the risk of PH remains controversial, it is thought that increased circulating serotonin, due to the inhibition of SERT-mediated serotonin reuptake or serotonin receptor-mediated serotonin release, were plausible mechanisms (Caccia et al., 1993; Rothman et al., 1999). Over a decade later, Morrell and colleagues reported that *Bmpr2* heterozygous mice exposed to serotonin displayed a greater susceptibility to the development of PH than wild type animals (Long et al., 2006). More recently, a meta-analysis of PAH genetic studies found that individuals harbouring polymorphisms in the gene encoding for SERT have a significantly greater risk of developing IPAH (Zhang et al., 2013). Although the exact mechanisms by which these polymorphisms may contribute the development of PAH is unknown, evidence from animals studies has demonstrated that transgenic mice overexpressing smooth muscle SERT spontaneously develop PH (Guignabert et al., 2006) and transgenic mice globally overexpressing SERT display more severe pulmonary vascular remodelling when exposed to hypoxia than wild type counterparts (MacLean et al., 2004). Thus, it would appear that alterations in SERT

activity and serotonin uptake might be one possible mechanism underlying the development of PAH.

Clinically, sertraline is prescribed to patients with PAH for the treatment of depression. To date, three retrospective studies have examined the use of SSRIs in patients with PAH. Interpreting the results of these studies is complicated by that fact that the effects of each SSRI are not reported individually, but instead SSRIs are reported as groups based on their affinity for SERT (i.e. "high-affinity" or "low-affinity"). Nevertheless, two of these studies reported a marked decreased in mortality rates for patients taking high-affinity SSRIs (Kawut et al., 2006; Shah et al., 2009), while the third reported that high-affinity SSRIs were associated with greater mortality and worsened clinical outcomes (Sadoughi et al., 2013). Given the potential therapeutic benefits, or potential risks, associated with the use of high-affinity SSRIs in PAH, the importance of further clinical studies cannot be understated.

As stated previously, sertraline has been shown to have a protective effect in the MCT rat model by inhibiting the expression of pulmonary artery SERT mRNA (Li et al., 2006). Similar results have also been observed with other SSRIs, such as fluoxetine, in both the MCT rat model and the hypoxic mouse model (Guignabert et al., 2005; Marcos et al., 2003; Wang et al., 2011b; Zhai et al., 2009). These findings have led to a renewed interest in targeting the serotonin pathway for the treatment of PAH (Thomas et al., 2013). Given that our *in vivo* evaluation of sertraline in the SU/CH model did not yield similar results to initial experiments performed in the MCT model, one might speculate that the difference in efficacy was due to the difference in animal models. As stated in the introduction, the SU/CH model is likely a better model of human PAH than the MCT

model, and therefore, our findings may more accurately predict the response of the human disease to sertraline. Also in contrast to Li et al, we chose to deliver sertraline via subcutaneous osmotic pumps rather than oral gavage which may have lead to differences in the metabolism and/or bioavailability of sertraline. While we did not perform pharmacokinetic experiments in the present study, the information gleaned from such investigations would have provided additional insight into the efficacy of our method of small molecule delivery. Alternatively, we could have analyzed the expression of known sertraline targets such as SERT.

5.5 Future Research Directions

Understanding the role of TCTP in the pathogenesis of PAH remains an important goal for future research. In addition to concluding our experiments utilizing TCTP small molecule inhibitors, future studies might benefit from utilizing more targeted approaches to down-regulate or inhibit TCTP. Specifically, the use of molecular silencing strategies (i.e. siRNA or shRNA) or pulmonary artery endothelial-specific transgenic knockout models would help circumvent issues associated with the use of small molecules such as lack of potency and unwanted off-target effects. The delivery of silencing molecules could potentially be achieved through *in vivo* transfection or viral-mediated transduction methods that specifically target pulmonary ECs. For example, in 2012 Morecroft and colleagues selectively knocked-down tryptophan hydrolase-1 (Tph1) in pulmonary ECs using shRNA guided by angiotensin-converting enzyme antibodies (Morecroft et al., 2012). Alternatively, our group, and others, have successfully delivered shRNA to the pulmonary endothelium using specialized cationic polymer transfection reagents

(Dungey, 2012; Kamlah et al., 2009; Wang et al., 2011a).

Aside from the direct manipulation of TCTP *in vivo,* it would also be worthwhile to further understand the role of TCTP as a survival factor in the context of vascular cell apoptosis *in vitro* (Sirois et al., 2011). As noted by Sirois and colleagues, TCTP is released from ECs undergoing apoptosis in exosome-like nanovesicles and can confer apoptosis-resistance to nearby smooth muscle cells (Sirois et al., 2011). As stated earlier, this may be a possible mechanism by which widespread pulmonary EC apoptosis contributes to the survival and proliferation of nearby pulmonary smooth muscle cells, ECs, or inflammatory cells in PAH. The release of TCTP by ECs undergoing apoptosis may also be a mechanism by which TCTP enters the systemic circulation. Accordingly, it was recently shown that TCTP levels are significantly elevated in patients with solid cancers following radiation or chemotherapies that induce widespread apoptosis (Sinthujaroen et al., 2014). Therefore, regardless of whether or not TCTP plays any role in lung arterial remodelling in PAH, it could potentially serve as a useful biomarker for EC apoptosis and allow us to study the molecular events in patients occurring during the earliest stages of disease progression.

5.6 Conclusions

Our *in vitro* findings in RLMVECs compliment previous reports demonstrating the ability to thioridazine to down-regulate TCTP and induce hallmarks of apoptosis in ECs. To the best of our knowledge, we are the first group to examine the efficacy of thioridazine as a PAH therapeutic and to evaluate sertraline in the SU/CH rat model. While our preliminary *in vivo* experiments did not give rise to any definitive results, we

believe that further studies examining thioridazine, sertraline, or other TCTP-specific molecular inhibition strategies in the SU/CH rat model of PAH are warranted. Moreover, given that sertraline is currently prescribed to patients with PAH, clinical studies exploring the effects of this small molecule may provide new insights into this challenging disease.

REFERENCES

Abe, K., Toba, M., Alzoubi, A., Ito, M., Fagan, K. A., Cool, C. D., . . . Oka, M. (2010). Formation of plexiform lesions in experimental severe pulmonary arterial hypertension. *Circulation, 121*(25), 2747-2754.

Amson, R., Pece, S., Marine, J. C., Di Fiore, P. P., & Telerman, A. (2013). TPT1/ TCTP-regulated pathways in phenotypic reprogramming. *Trends Cell Biol, 23*(1), 37-46.

Amson, R., Pece, S., Lespagnol, A., Vyas, R., Mazzarol, G., Tosoni, D., . . . Telerman, A. (2012). Reciprocal repression between P53 and TCTP. *Nat Med, 18*(1), 91-99.

Archer, S. L., Weir, E. K., & Wilkins, M. R. (2010). Basic science of pulmonary arterial hypertension for clinicians: new concepts and experimental therapies. *Circulation, 121*(18), 2045-2066.

Asahara, T., Murohara, T., Sullivan, A., Silver, M., van der Zee, R., Li, T., . . . Isner, J. M. (1997). Isolation of putative progenitor endothelial cells for angiogenesis. *Science, 275*(5302), 964-967.

Atkinson, C., Stewart, S., Upton, P. D., Machado, R., Thomson, J. R., Trembath, R. C., & Morrell, N. W. (2002). Primary pulmonary hypertension is associated with reduced pulmonary vascular expression of type II bone morphogenetic protein receptor. *Circulation, 105*(14), 1672-1678.

Austin, E. D., Ma, L., LeDuc, C., Berman Rosenzweig, E., Borczuk, A., Phillips, J. A., 3rd, . . . Chung, W. K. (2012). Whole exome sequencing to identify a novel gene (caveolin-1) associated with human pulmonary arterial hypertension. *Circ Cardiovasc Genet, 5*(3), 336-343.

Barst, R. J., McGoon, M., Torbicki, A., Sitbon, O., Krowka, M. J., Olschewski, H., & Gaine, S. (2004). Diagnosis and differential assessment of pulmonary arterial hypertension. *J Am Coll Cardiol, 43*(12 Suppl S), 40s-47s.

Benza, R. L., Miller, D. P., Barst, R. J., Badesch, D. B., Frost, A. E., & McGoon, M. D. (2012). An evaluation of long-term survival from time of diagnosis in pulmonary arterial hypertension from the REVEAL Registry. *Chest, 142*(2), 448-456.

Bommer, U. A., & Thiele, B. J. (2004). The translationally controlled tumour protein (TCTP). *Int J Biochem Cell Biol, 36*(3), 379-385.

Budhiraja, R., Tuder, R. M., & Hassoun, P. M. (2004). Endothelial dysfunction in pulmonary hypertension. *Circulation, 109*(2), 159-165.

Byun, H. J., Lee, J. H., Kim, B. R., Kang, S., Dong, S. M., Park, M. S., . . . Rho, S. B. (2012). Anti-angiogenic effects of thioridazine involving the FAK-mTOR pathway. *Microvasc Res, 84*(3), 227-234.

Caccia, S., Anelli, M., Ferrarese, A., Fracasso, C., & Garattini, S. (1993). The role of d-norfenfluramine in the indole-depleting effect of d-fenfluramine in the rat. *Eur J Pharmacol, 233*(1), 71-77.

Campo, A., Mathai, S. C., Le Pavec, J., Zaiman, A. L., Hummers, L. K., Boyce, D., . . . Hassoun, P. M. (2011). Outcomes of hospitalisation for right heart failure in pulmonary arterial hypertension. *Eur Respir J, 38*(2), 359-367.

Chaouat, A., Coulet, F., Favre, C., Simonneau, G., Weitzenblum, E., Soubrier, F., & Humbert, M. (2004). Endoglin germline mutation in a patient with hereditary haemorrhagic telangiectasia and dexfenfluramine associated pulmonary arterial hypertension. *Thorax, 59*(5), 446-448.

Cho, Y., Maeng, J., Ryu, J., Shin, H., Kim, M., Oh, G. T., . . . Lee, K. (2012). Hypertension resulting from overexpression of translationally controlled tumor protein increases the severity of atherosclerosis in apolipoprotein E knock-out mice. *Transgenic Res, 21*(6), 1245-1254.

Christman, B. W., McPherson, C. D., Newman, J. H., King, G. A., Bernard, G. R., Groves, B. M., & Loyd, J. E. (1992). An imbalance between the excretion of thromboxane and prostacyclin metabolites in pulmonary hypertension. *N Engl J Med, 327*(2), 70-75.

Clozel, M., Gray, G. A., Breu, V., Loffler, B. M., & Osterwalder, R. (1992). The endothelin ETB receptor mediates both vasodilation and vasoconstriction in vivo. *Biochem Biophys Res Commun, 186*(2), 867-873.

Cool, C. D., Stewart, J. S., Werahera, P., Miller, G. J., Williams, R. L., Voelkel, N. F., & Tuder, R. M. (1999). Three-dimensional reconstruction of pulmonary arteries in plexiform pulmonary hypertension using cell-specific markers. Evidence for a dynamic and heterogeneous process of pulmonary endothelial cell growth. *Am J Pathol, 155*(2), 411-419.

D'Alonzo, G. E., Barst, R. J., Ayres, S. M., Bergofsky, E. H., Brundage, B. H., Detre, K. M., . . . et al. (1991). Survival in patients with primary pulmonary hypertension. Results from a national prospective registry. *Ann Intern Med, 115*(5), 343-349.

Dahal, B.K., Kosanovic, D., Kaulen, C., Cornitescu, T., Savai, R., Hoffmann, J., Reiss, I., … Schermuly, R.T. (2011). Involvement of mast cells in monocrotaline-induced pulmonary hypertension in rats. *Respir Res, 12(60).*

de Jesus Perez, V. A., Yuan, K., Lyuksyutova, M. A., Dewey, F., Orcholski, M. E., Shuffle, E. M., . . . Zamanian, R. T. (2014). Whole-exome sequencing reveals TopBP1 as a novel gene in idiopathic pulmonary arterial hypertension. *Am J Respir Crit Care Med, 189*(10), 1260-1272.

Demolli, S. S., K.; Doddaballapur, A,; Boon, R.A.; Doebele, C.; Eckert, A.; et al. . (2013). Shear Stress-Regulated Mir-27a/b Controls Pericyte Recruitment: Implications for Vessel Maturation. *Circulation*, 128.

Drake, K. M., Zygmunt, D., Mavrakis, L., Harbor, P., Wang, L., Comhair, S. A., . . . Aldred, M. A. (2011). Altered MicroRNA processing in heritable pulmonary arterial hypertension: an important role for Smad-8. *Am J Respir Crit Care Med, 184*(12), 1400-1408.

Dungey, A. A. (2012) Characterization and role of krüppel-like factor 2 in models of pulmonary hypertension (Doctoral thesis). Retreieved from http://hdl.handle.net/1807/32701

Eap, C. B., Guentert, T. W., Schaublin-Loidl, M., Stabl, M., Koeb, L., Powell, K., & Baumann, P. (1996). Plasma levels of the enantiomers of thioridazine, thioridazine 2-sulfoxide, thioridazine 2-sulfone, and thioridazine 5-sulfoxide in poor and extensive metabolizers of dextromethorphan and mephenytoin. *Clin Pharmacol Ther, 59*(3), 322-331.

Foster, W.S., Suen, C.M., & Stewart, D.J. (2014) Regenerative cell and tissue-based therapies for the treatment of pulmonary arterial hypertension. *Can J Cardiol. 30*(11)*,* 1150-1160.

Farkas, D., Kraskauskas, D., Drake, J. I., Alhussaini, A. A., Kraskauskiene, V., Bogaard, H. J., . . . Farkas, L. (2014). CXCR4 inhibition ameliorates severe obliterative pulmonary hypertension and accumulation of C-kit(+) cells in rats. *PLoS One, 9*(2), e89810.

Gatfield, J., Mueller Grandjean, C., Sasse, T., Clozel, M., & Nayler, O. (2012). Slow receptor dissociation kinetics differentiate macitentan from other endothelin receptor antagonists in pulmonary arterial smooth muscle cells. *PLoS One, 7*(10), e47662.

Giaid, A., & Saleh, D. (1995). Reduced expression of endothelial nitric oxide synthase in the lungs of patients with pulmonary hypertension. *N Engl J Med, 333*(4), 214-221.

Giaid, A., Yanagisawa, M., Langleben, D., Michel, R. P., Levy, R., Shennib, H., . . . Stewart, D. J. (1993). Expression of endothelin-1 in the lungs of patients with pulmonary hypertension. *N Engl J Med, 328*(24), 1732-1739.

Gomez-Arroyo, J. G., Farkas, L., Alhussaini, A. A., Farkas, D., Kraskauskas, D., Voelkel, N. F., & Bogaard, H. J. (2012). The monocrotaline model of pulmonary hypertension in perspective. *Am J Physiol Lung Cell Mol Physiol, 302*(4), L363-369.

Guignabert, C., Izikki, M., Tu, L. I., Li, Z., Zadigue, P., Barlier-Mur, A. M., . . . Eddahibi, S. (2006). Transgenic mice overexpressing the 5-hydroxytryptamine transporter gene in smooth muscle develop pulmonary hypertension. *Circ Res, 98*(10), 1323-1330.

Guignabert, C., Raffestin, B., Benferhat, R., Raoul, W., Zadigue, P., Rideau, D., . . . Eddahibi, S. (2005). Serotonin transporter inhibition prevents and reverses monocrotaline-induced pulmonary hypertension in rats. *Circulation, 111*(21), 2812-2819.

Haduch, A., Wojcikowski, J., & Daniel, W. A. (2007). The activity of cytochrome P450 CYP2B in rat liver during neuroleptic treatment. *Pharmacol Rep, 59*(5), 606-612.

Harrison, R. E., Flanagan, J. A., Sankelo, M., Abdalla, S. A., Rowell, J., Machado, R. E., . . . Trembath, R. C. (2003). Molecular and functional analysis identifies ALK-1 as the predominant cause of pulmonary hypertension related to hereditary haemorrhagic telangiectasia. *J Med Genet, 40*(12), 865-871.

Hatano, S., Toma, S., & World Health Organization. (1975). Primary pulmonary hypertension: report on a WHO meeting, Geneva, 15-17 October 1973 (Vol. 146, pp. 45). Geneva: World Health Organization.

Hoff, P. M., Wolff, R. A., Bogaard, K., Waldrum, S., & Abbruzzese, J. L. (2006). A Phase I study of escalating doses of the tyrosine kinase inhibitor semaxanib (SU5416) in combination with irinotecan in patients with advanced colorectal carcinoma. *Jpn J Clin Oncol, 36*(2), 100-103.

Humbert, M., Lau, E. M., Montani, D., Jais, X., Sitbon, O., & Simonneau, G. (2014). Advances in therapeutic interventions for patients with pulmonary arterial hypertension. *Circulation, 130*(24), 2189-2208.

Ingram, D. A., Caplice, N. M., & Yoder, M. C. (2005). Unresolved questions, changing definitions, and novel paradigms for defining endothelial progenitor cells. *Blood, 106*(5), 1525-1531.

Ingram, D. A., Mead, L. E., Tanaka, H., Meade, V., Fenoglio, A., Mortell, K., . . . Yoder, M. C. (2004). Identification of a novel hierarchy of endothelial progenitor cells using human peripheral and umbilical cord blood. *Blood, 104*(9), 2752-2760.

Jiang, B., Deng, Y., Suen, C., Taha, M., Chaudhary, K. R., Courtman, D. W., & Stewart, D. J. (2015). Marked Strain-specific Differences in the SU5416 Rat Model of Severe Pulmonary Arterial Hypertension. *Am J Respir Cell Mol Biol*.

Jones, D. A., Benjamin, C. W., & Linseman, D. A. (1995). Activation of thromboxane and prostacyclin receptors elicits opposing effects on vascular smooth muscle cell growth and mitogen-activated protein kinase signaling cascades. *Mol Pharmacol, 48*(5), 890-896.

Jung, J., Kim, H.Y., Maeng, J., Kim, M., Shin, D.H, Lee, K. (2014) Interaction of translationally controlled tumor protein with Apaf-1 is involved in the development of chemoresistance in HeLa cells. *BMC Cancer*, *7(14),* 165.

Jurasz, P., Courtman, D., Babaie, S., & Stewart, D. J. (2010). Role of apoptosis in pulmonary hypertension: from experimental models to clinical trials. *Pharmacol Ther, 126*(1), 1-8.

Kamlah, F., Eul, B. G., Li, S., Lang, N., Marsh, L. M., Seeger, W., . . . Hanze, J. (2009). Intravenous injection of siRNA directed against hypoxia-inducible factors prolongs survival in a Lewis lung carcinoma cancer model. *Cancer Gene Ther, 16*(3), 195-205.

Kashiwakura, J. C., Ando, T., Matsumoto, K., Kimura, M., Kitaura, J., Matho, M. H., . . . Kawakami, T. (2012). Histamine-releasing factor has a proinflammatory role in mouse models of asthma and allergy. *J Clin Invest, 122*(1), 218-228.

Kawut, S. M., Horn, E. M., Berekashvili, K. K., Lederer, D. J., Widlitz, A. C., Rosenzweig, E. B., & Barst, R. J. (2006). Selective serotonin reuptake inhibitor use and outcomes in pulmonary arterial hypertension. *Pulm Pharmacol Ther, 19*(5), 370-374.

Kay, J. M., Harris, P., & Heath, D. (1967). Pulmonary hypertension produced in rats by ingestion of Crotalaria spectabilis seeds. *Thorax, 22*(2), 176-179.

Kim, M. J., Kwon, J.S., Suh, S. H., Suh, J. K., Jung, J., Lee, S.N., . . . Lee, K. (2008) Transgenic overexpression of translationally controlled tumor protein induces systemic hypertension via repression of Na+,K+-ATPase. *J Mol Cell Cardiol, 44*(1),151-159.

Kim, N. H., & Rubin, L. J. (2002). Endothelin in health and disease: endothelin receptor antagonists in the management of pulmonary artery hypertension. *J Cardiovasc Pharmacol Ther, 7*(1), 9-19.

Kirchner, V., Kelly, C. A., & Harvey, R. J. (2001). Thioridazine for dementia. *Cochrane Database Syst Rev*(3), Cd000464.

Koide, Y., Kiyota, T., Tonganunt, M., Pinkaew, D., Liu, Z., Kato, Y., . . .Fujise, K. (2009). Embryonic lethality of fortilin-null mutant mice by BMP-pathway overactivation. *Biochim Biophys Acta, 1790*(5), 326-338.

Lavoie, J. R., Ormiston, M. L., Perez-Iratxeta, C., Courtman, D. W., Jiang, B., Ferrer, E., . . . Stewart, D. J. (2014). Proteomic analysis implicates translationally controlled tumor protein as a novel mediator of occlusive vascular remodeling in pulmonary arterial hypertension. *Circulation, 129*(21), 2125-2135.

Lee, S. D., Shroyer, K. R., Markham, N. E., Cool, C. D., Voelkel, N. F., & Tuder, R. M. (1998). Monoclonal endothelial cell proliferation is present in primary but not secondary pulmonary hypertension. *J Clin Invest, 1;101*(5), 927-934.

Levy, M., Maurey, C., Celermajer, D. S., Vouhe, P. R., Danel, C., Bonnet, D., & Israel-Biet, D. (2007). Impaired apoptosis of pulmonary endothelial cells is associated with intimal proliferation and irreversibility of pulmonary hypertension in congenital heart disease. *J Am Coll Cardiol, 49*(7), 803-810.

Li, F., Zhang, D., & Fujise, K. (2001). Characterization of fortilin, a novel antiapoptotic protein. *J Biol Chem, 276*(50), 47542-47549.

Li, M., Vattulainen, S., Aho, J., Orcholski, M., Rojas, V., Yuan, K., . . . Alastalo, T. P. (2014). Loss of bone morphogenetic protein receptor 2 is associated with abnormal DNA repair in pulmonary arterial hypertension. *Am J Respir Cell Mol Biol, 50*(6), 1118-1128.

Li, X. Q., Hong, Y., Wang, Y., Zhang, X. H., & Wang, H. L. (2006). Sertraline protects against monocrotaline-induced pulmonary hypertension in rats. *Clin Exp Pharmacol Physiol, 33*(11), 1047-1051.

Lin, G., Hawes, E. M., McKay, G., Korchinski, E. D., & Midha, K. K. (1993). Metabolism of piperidine-type phenothiazine antipsychotic agents. IV. Thioridazine in dog, man and rat. *Xenobiotica, 23*(10), 1059-1074.

Lo, W. Y., Wang, H. J., Chiu, C. W., & Chen, S. F. (2012). miR-27b-regulated TCTP as a novel plasma biomarker for oral cancer: from quantitative proteomics to post-transcriptional study. *J Proteomics, 77*, 154-166.

Long, L., MacLean, M. R., Jeffery, T. K., Morecroft, I., Yang, X., Rudarakanchana, N., . . . Morrell, N. W. (2006). Serotonin increases susceptibility to pulmonary hypertension in BMPR2-deficient mice. *Circ Res, 98*(6), 818-827.

Lundmark, J., Reis, M., & Bengtsson, F. (2000). Therapeutic drug monitoring of sertraline: variability factors as displayed in a clinical setting. *Ther Drug Monit*, 22(4)*,* 446-54.

Ma, L., Roman-Campos, D., Austin, E. D., Eyries, M., Sampson, K. S., Soubrier, F., . . . Chung, W. K. (2013). A novel channelopathy in pulmonary arterial hypertension. *N Engl J Med, 369*(4), 351-361.

Maarman, G., Lecour, S., Butrous, G., Thienemann, F., & Sliwa, K. (2013). A comprehensive review: the evolution of animal models in pulmonary hypertension research; are we there yet? *Pulm Circ, 3*(4), 739-756.

MacDonald, S. M., Rafnar, T., Langdon, J., & Lichtenstein, L. M. (1995). Molecular identification of an IgE-dependent histamine-releasing factor. *Science, 269*(5224), 688-690.

Machado, R. D., Eickelberg, O., Elliott, C. G., Geraci, M. W., Hanaoka, M., Loyd, J. E., . . . Chung, W. K. (2009). Genetics and genomics of pulmonary arterial hypertension. *J Am Coll Cardiol, 54*(1 Suppl), S32-42.

MacLean, M. R. (2007). Pulmonary hypertension and the serotonin hypothesis: where are we now? *Int J Clin Pract Suppl*(156), 27-31.

MacLean, M. R., Deuchar, G. A., Hicks, M. N., Morecroft, I., Shen, S., Sheward, J., . . . Harmar, A. (2004). Overexpression of the 5-hydroxytryptamine transporter gene: effect on pulmonary hemodynamics and hypoxia-induced pulmonary hypertension. *Circulation, 109*(17), 2150-2155.

Maj, J., Mogilnicka, E., & Kordecka, A. (1979). Chronic treatment with antidepressant drugs: potentiation of apomorphine-induced aggressive behaviour in rats. *Neurosci Lett, 13*(3), 337-341.

Makowski, C. T., Rissmiller, R. W., & Bullington, W. M. (2015). Riociguat: a novel new drug for treatment of pulmonary hypertension. *Pharmacotherapy, 35*(5), 502-519.

Marcos, E., Adnot, S., Pham, M. H., Nosjean, A., Raffestin, B., Hamon, M., & Eddahibi, S. (2003). Serotonin transporter inhibitors protect against hypoxic pulmonary hypertension. *Am J Respir Crit Care Med, 168*(4), 487-493.

Masaki, T., Miwa, S., Sawamura, T., Ninomiya, H., & Okamoto, Y. (1999). Subcellular mechanisms of endothelin action in vascular system. *Eur J Pharmacol, 375*(1-3), 133-138.

Mason, N. A., Springall, D. R., Burke, M., Pollock, J., Mikhail, G., Yacoub, M. H., & Polak, J. M. (1998). High expression of endothelial nitric oxide synthase in plexiform lesions of pulmonary hypertension. *J Pathol, 185*(3), 313-318.

Masri, F. A., Xu, W., Comhair, S. A., Asosingh, K., Koo, M., Vasanji, A., . . . Erzurum, S. C. (2007). Hyperproliferative apoptosis-resistant endothelial cells in idiopathic

pulmonary arterial hypertension. *Am J Physiol Lung Cell Mol Physiol, 293*(3), L548-554.

McLaughlin, V. V., & McGoon, M. D. (2006). Pulmonary arterial hypertension. *Circulation, 114*(13), 1417-1431.

McMurtry, M. S., Archer, S. L., Altieri, D. C., Bonnet, S., Haromy, A., Harry, G., . . . Michelakis, E. D. (2005). Gene therapy targeting survivin selectively induces pulmonary vascular apoptosis and reverses pulmonary arterial hypertension. *J Clin Invest, 115*(6), 1479-1491.

Melis, V., Usach, I., & Peris, J.E. (2012) Determination of sertraline in rat plasma by HPLC and fluorescence detection and its application to in vivo pharmacokinetic studies. *J Sep Sci, 35(23)*, 3302-7.

Miyazono, K., Maeda, S., & Imamura, T. (2005). BMP receptor signaling: transcriptional targets, regulation of signals, and signaling cross-talk. *Cytokine Growth Factor Rev, 16*(3), 251-263.

Morecroft, I., White, K., Caruso, P., Nilsen, M., Loughlin, L., Alba, R., . . . Maclean, M. R. (2012). Gene therapy by targeted adenovirus-mediated knockdown of pulmonary endothelial Tph1 attenuates hypoxia-induced pulmonary hypertension. *Mol Ther, 20*(8), 1516-1528.

Mouraret, N., Marcos, E., Abid, S., Gary-Bobo, G., Saker, M., Houssaini, A., . . . Adnot, S. (2013). Activation of lung p53 by Nutlin-3a prevents and reverses experimental pulmonary hypertension. *Circulation, 127*(16), 1664-1676.

Murdoch, D., & McTavish, D. (1992) Sertraline. A review of its pharmacodynamic and pharmacokinetic properties, and therapeutic potential in depression and obsessive-compulsive disorder. *Drugs*, *44(4)*, 604-24.

Nasim, M. T., Ogo, T., Ahmed, M., Randall, R., Chowdhury, H. M., Snape, K. M., . . . Machado, R. D. (2011) Molecular genetic characterization of SMAD signaling molecules in pulmonary arterial hypertension. *Human Mutat, 32*(12), 1385-1389.

Neylon, C. B., Avdonin, P. V., Dilley, R. J., Larsen, M. A., Tkachuk, V. A., & Bobik, A. (1994). Different electrical responses to vasoactive agonists in morphologically distinct smooth muscle cell types. *Circ Res, 75*(4), 733-741.

O'Donnell, A., Padhani, A., Hayes, C., Kakkar, A. J., Leach, M., Trigo, J. M., . . . Judson, I. (2005). A Phase I study of the angiogenesis inhibitor SU5416 (semaxanib) in solid tumours, incorporating dynamic contrast MR pharmacodynamic end points. *Br J Cancer, 93*(8), 876-883.

Ohta-Ogo, K., Hao, H., Ishibashi-Ueda, H., Hirota, S., Nakamura, K., Ohe, T., & Ito, H. (2012). CD44 expression in plexiform lesions of idiopathic pulmonary arterial hypertension. *Pathol Int, 62*(4), 219-225.

Okada, K., Tanaka, Y., Bernstein, M., Zhang, W., Patterson, G. A., & Botney, M. D. (1997). Pulmonary hemodynamics modify the rat pulmonary artery response to injury. A neointimal model of pulmonary hypertension. *Am J Pathol, 151*(4), 1019-1025.

Otsuki, S., Sawada, H., Yodoya, N., Shinohara, T., Kato, T., Ohashi, H., …Mitani, Y. (2015). Potential contribution of phenotypically modulated smooth muscle cells and related inflammation in the development of experimental obstructive pulmonary vasculopathy in rats. *PLoS Onel, 24;10*.

Paffett, M. L., Hesterman, J., Candelaria, G., Lucas, S., Anderson, T., Irwin, D., . . . Campen, M. J. (2012). Longitudinal in vivo SPECT/CT imaging reveals morphological changes and cardiopulmonary apoptosis in a rodent model of pulmonary arterial hypertension. *PLoS One, 7*(7), e40910.

Park, M. S., Dong, S. M., Kim, B. R., Seo, S. H., Kang, S., Lee, E. J., . . . Rho, S. B. (2014). Thioridazine inhibits angiogenesis and tumor growth by targeting the VEGFR-2/PI3K/mTOR pathway in ovarian cancer xenografts. *Oncotarget, 5*(13), 4929-4934.

Perrin, S., Chaumais, M. C., O'Connell, C., Amar, D., Savale, L., Jais, X., . . . Sitbon, O. (2015). New pharmacotherapy options for pulmonary arterial hypertension. *Expert Opin Pharmacother*, 1-19.

Pinkaew, D., Le, R. J., Chen, Y., Eltorky, M., Teng, B. B., & Fujise, K. (2013). Fortilin reduces apoptosis in macrophages and promotes atherosclerosis. *Am J Physiol Heart Circ Physiol, 305*(10), H1519-1529.

Price, L. C., Wort, S. J., Perros, F., Dorfmuller, P., Huertas, A., Montani, D., . . . Humbert, M. (2012). Inflammation in pulmonary arterial hypertension. *Chest, 141*(1), 210-221.

Pullamsetti, S. S., Schermuly, R., Ghofrani, A., Weissmann, N., Grimminger, F., & Seeger, W. (2014). Novel and emerging therapies for pulmonary hypertension. *Am J Respir Crit Care Med, 189*(4), 394-400.

Rai, P. R., Cool, C. D., King, J. A., Stevens, T., Burns, N., Winn, R. A., . . . Voelkel, N. F. (2008). The cancer paradigm of severe pulmonary arterial hypertension. *Am J Respir Crit Care Med, 178*(6), 558-564.

Roth, B., Driscol, J. . (2011). PDSP Ki Database. Retrieved from University of North Carolina at Chapel Hill and the United States National Institute of Mental Health.

Rothman, R. B., Ayestas, M. A., Dersch, C. M., & Baumann, M. H. (1999). Aminorex, fenfluramine, and chlorphentermine are serotonin transporter substrates. Implications for primary pulmonary hypertension. *Circulation, 100*(8), 869-875.

Ryan, J. J., Bloch, K., & Archer, S. L. (2011). Rodent models of pulmonary hypertension: harmonization with the world heath organizations's categorization of human PH. *Int J Clin Pract Suppl,* (172), 15-34.

Ryan, J. J., & Archer, S. L. (2014). The right ventricle in pulmonary arterial hypertension: disorders of metabolism, angiogenesis and adrenergic signaling in right ventricular failure. *Circ Res, 115*(1), 176-188.

Sadoughi, A., Roberts, K. E., Preston, I. R., Lai, G. P., McCollister, D. H., Farber, H. W., & Hill, N. S. (2013). Use of selective serotonin reuptake inhibitors and outcomes in pulmonary arterial hypertension. *Chest, 144*(2), 531-541.

Sakao, S., Tatsumi, K., & Voelkel, N. F. (2009). Endothelial cells and pulmonary arterial hypertension: apoptosis, proliferation, interaction and transdifferentiation. *Respir Res, 10*, 95.

Savai, R., Pullamesetti, S.S., Kolbe, J., Bieniek, E., Voswinckel, R., Fink, L., … et al. (2009). Immune and inflammatory cell involvement in the pathology of idiopathic pulmonary arterial hypertension. *Am J Respir Crit Care Med, 186(9)*, 897–908.

Schmierer, B., & Hill, C. S. (2007). TGFbeta-SMAD signal transduction: molecular specificity and functional flexibility. *Nat Rev Mol Cell Biol, 8*(12), 970-982.

Seeman, P. (1990). Atypical neuroleptics: role of multiple receptors, endogenous dopamine, and receptor linkage. *Acta Psychiatr Scand Suppl, 358*, 14-20.

Shah, M., Patel, K., & Sehgal, P. B. (2005). Monocrotaline pyrrole-induced endothelial cell megalocytosis involves a Golgi blockade mechanism. *Am J Physiol Cell Physiol, 288*(4), C850-862.

Shah, S. J., Gomberg-Maitland, M., Thenappan, T., & Rich, S. (2009). Selective serotonin reuptake inhibitors and the incidence and outcome of pulmonary hypertension. *Chest, 136*(3), 694-700.

Shi, R., Zhang, Y., Shi, Y., Shi, S., & Jiang, L. (2012). Inhibition of peroxisomal beta-oxidation by thioridazine increases the amount of VLCFAs and Abeta generation in the rat brain. *Neurosci Lett, 528*(1), 6-10.f

Simonneau, G., Galie, N., Rubin, L. J., Langleben, D., Seeger, W., Domenighetti, G., . . . Fishman, A. (2004). Clinical classification of pulmonary hypertension. *J Am Coll Cardiol, 43*(12 Suppl S), 5s-12s.

Simonneau, G., Gatzoulis, M. A., Adatia, I., Celermajer, D., Denton, C., Ghofrani, A., . . . Souza, R. (2013). Updated clinical classification of pulmonary hypertension. *J Am Coll Cardiol, 62*(25 Suppl), D34-41.

Sinthujaroen, P., Wanachottrakul, N., Pinkaew, D., Petersen, J. R., Phongdara, A., Sheffield-Moore, M., & Fujise, K. (2014). Elevation of serum fortilin levels is specific for apoptosis and signifies cell death in vivo. *BBA Clin, 2*, 103-111.

Sirois, I., Raymond, M. A., Brassard, N., Cailhier, J. F., Fedjaev, M., Hamelin, K., . . . Hebert, M. J. (2011). Caspase-3-dependent export of TCTP: a novel pathway for antiapoptotic intercellular communication. *Cell Death Differ, 18*(3), 549-562. doi: 10.1038/cdd.2010.126

Sitbon, O., Channick, R., Chin, K. M., Frey, A., Gaine, S., Galie, N., . . . McLaughlin, V. V. (2015). Selexipag for the Treatment of Pulmonary Arterial Hypertension. *N Engl J Med, 373*(26), 2522-2533.

Sitbon, O., Humbert, M., Jais, X., Ioos, V., Hamid, A. M., Provencher, S., . . . Simonneau, G. (2005). Long-term response to calcium channel blockers in idiopathic pulmonary arterial hypertension. *Circulation, 111*(23), 3105-3111.

Stacher, E., Graham, B. B., Hunt, J.M., Gandjeva, A., Groshong, S. D., McLaughlin, V. V., . . .Tuder, R. M. (2012). Modern age pathology of pulmonary arterial hypertension. *Am J Respir Crit Care Med, 1;186*(3), 261-272.

Stasch, J. P., Pacher, P., & Evgenov, O. V. (2011). Soluble guanylate cyclase as an emerging therapeutic target in cardiopulmonary disease. *Circulation, 123*(20), 2263-2273.

Stenmark, K. R., Meyrick, B., Galie, N., Mooi, W. J., & McMurtry, I. F. (2009). Animal models of pulmonary arterial hypertension: the hope for etiological discovery and pharmacological cure. *Am J Physiol Lung Cell Mol Physiol, 297*(6), L1013-1032.

Stewart, D. J., Levy, R. D., Cernacek, P., & Langleben, D. (1991). Increased plasma endothelin-1 in pulmonary hypertension: marker or mediator of disease? *Ann Intern Med, 114*(6), 464-469.

Stollberger, C., Huber, J. O., & Finsterer, J. (2005). Antipsychotic drugs and QT prolongation. *Int Clin Psychopharmacol, 20*(5), 243-251.

Susini, L., Besse, S., Duflaut, D., Lespagnol, A., Beekman, C., Fiucci, G., . . . Telerman, A. (2008). TCTP protects from apoptotic cell death by antagonizing bax function. *Cell Death Differ, 15*(8), 1211-1220.

Taraseviciene-Stewart, L., Kasahara, Y., Alger, L., Hirth, P., Mc Mahon, G., Waltenberger, J., . . . Tuder, R. M. (2001). Inhibition of the VEGF receptor 2 combined with chronic hypoxia causes cell death-dependent pulmonary endothelial cell proliferation and severe pulmonary hypertension. *Faseb j, 15*(2), 427-438.

Tei, C., Dujardin, K. S., Hodge, D. O., Bailey, K. R., McGoon, M. D., Tajik, A. J., & Seward, S. B. (1996). Doppler echocardiographic index for assessment of global right ventricular function. *J Am Soc Echocardiogr, 9*(6), 838-847.

Teichert-Kuliszewska, K., Kutryk, M. J., Kuliszewski, M. A., Karoubi, G., Courtman, D. W., Zucco, L., . . . Stewart, D. J. (2006). Bone morphogenetic protein receptor-2 signaling promotes pulmonary arterial endothelial cell survival: implications for loss-of-function mutations in the pathogenesis of pulmonary hypertension. *Circ Res, 98*(2), 209-217.

Telerman, A., & Amson, R. (2009). The molecular programme of tumour reversion: the steps beyond malignant transformation. *Nat Rev Cancer, 9*(3), 206-216.

Thomas, G., Thomas, G., & Luther, H. (1981). Transcriptional and translational control of cytoplasmic proteins after serum stimulation of quiescent Swiss 3T3 cells. *Proc Natl Acad Sci U S A, 78*(9), 5712-5716.

Thomas, M., Ciuclan, L., Hussey, M. J., & Press, N. J. (2013). Targeting the serotonin pathway for the treatment of pulmonary arterial hypertension. *Pharmacol Ther, 138*(3), 409-417.

Toba, M., Alzoubi, A., O'Neill, K. D., Gairhe, S., Matsumoto, Y., Oshima, K., . . . McMurtry, I. F. (2014). Temporal hemodynamic and histological progression in Sugen5416/hypoxia/normoxia-exposed pulmonary arterial hypertensive rats. *Am J Physiol Heart Circ Physiol, 306*(2), H243-250.

Tuder, R. M., Chacon, M., Alger, L., Wang, J., Taraseviciene-Stewart, L., Kasahara, Y., . . . Voelkel, N. F. (2001). Expression of angiogenesis-related molecules in plexiform lesions in severe pulmonary hypertension: evidence for a process of disordered angiogenesis. *J Pathol, 195*(3), 367-374.

Tuder, R. M., Cool, C. D., Geraci, M. W., Wang, J., Abman, S. H., Wright, L., . . . Voelkel, N. F. (1999). Prostacyclin synthase expression is decreased in lungs from patients with severe pulmonary hypertension. *Am J Respir Crit Care Med, 159*(6), 1925-1932.

Tuder, R. M., Groves, B., Badesch, D. B., & Voelkel, N. F. (1994). Exuberant endothelial cell growth and elements of inflammation are present in plexiform lesions of pulmonary hypertension. *Am J Pathol, 144*(2), 275-285.

Tuynder, M., Fiucci, G., Prieur, S., Lespagnol, A., Geant, A., Beaucourt, S., . . . Telerman, A. (2004). Translationally controlled tumor protein is a target of tumor reversion. *Proc Natl Acad Sci U S A, 101*(43), 15364-15369.

Tuynder, M., Susini, L., Prieur, S., Besse, S., Fiucci, G., Amson, R., & Telerman, A. (2002). Biological models and genes of tumor reversion: cellular reprogramming through tpt1/TCTP and SIAH-1. *Proc Natl Acad Sci U S A, 99*(23), 14976-14981.

Urboniene, D., Haber, I., Fang, Y. H., Thenappan, T., & Archer, S. L. (2010). Validation of high-resolution echocardiography and magnetic resonance imaging vs. high-fidelity catheterization in experimental pulmonary hypertension. *Am J Physiol Lung Cell Mol Physiol, 299*(3), L401-412.

Voelkel, N. F., Quaife, R. A., Leinwand, L. A., Barst, R. J., McGoon, M. D., Meldrum, D. R., . . . Gail, D. B. (2006). Right ventricular function and failure: report of a National Heart, Lung, and Blood Institute working group on cellular and molecular mechanisms of right heart failure. *Circulation, 114*(17), 1883-1891.

Wang, R., Xu, Y. J., Liu, X. S., Zeng, D. X., & Xiang, M. (2011a). Knockdown of connective tissue growth factor by plasmid-based short hairpin RNA prevented pulmonary vascular remodeling in cigarette smoke-exposed rats. *Arch Biochem Biophys, 508*(1), 93-100.

Wang, Y., Zhang, X. H., & Wang, H. L. (2011b). Involvement of BMPR2 in the protective effect of fluoxetine against monocrotaline-induced endothelial apoptosis in rats. *Can J Physiol Pharmacol, 89*(5), 345-354.

White, R. J., Meoli, D. F., Swarthout, R. F., Kallop, D. Y., Galaria, II, Harvey, J. L., . . . Taubman, M. B. (2007). Plexiform-like lesions and increased tissue factor expression in a rat model of severe pulmonary arterial hypertension. *Am J Physiol Lung Cell Mol Physiol, 293*(3), L583-590.

Wojcikowski, J., & Daniel, W. A. (2002). Thioridazine-fluoxetine interaction at the level of the distribution process in vivo. *Pol J Pharmacol, 54*(6), 647-654.

Yeager, M. E., Halley, G. R., Golpon, H. A., Voelkel, N. F., & Tuder, R. M. (2001). Microsatellite instability of endothelial cell growth and apoptosis genes within plexiform lesions in primary pulmonary hypertension. *Circ Res, 19;88*(1), E2-E11.

Yildiz, A., Gönül A.S., & Tamam, L. (2002). Mechanism of Actions of Antidepressants: Beyond the Receptors. *Bull Clin Phychopharmacol, 12(4),* 194-200.

Zhai, F. G., Zhang, X. H., & Wang, H. L. (2009). Fluoxetine protects against monocrotaline-induced pulmonary arterial hypertension: potential roles of induction of apoptosis and upregulation of Kv1.5 channels in rats. *Clin Exp Pharmacol Physiol, 36*(8), 850-856.

Zhang, H., Xu, M., Xia, J., & Qin, R. Y. (2013). Association between serotonin transporter (SERT) gene polymorphism and idiopathic pulmonary arterial hypertension: a meta-analysis and review of the literature. *Metabolism, 62*(12), 1867-1875.

Zhao, Y. D., Courtman, D. W., Deng, Y., Kugathasan, L., Zhang, Q., & Stewart, D. J. (2005). Rescue of monocrotaline-induced pulmonary arterial hypertension using bone marrow-derived endothelial-like progenitor cells: efficacy of combined cell and eNOS gene therapy in established disease. *Circ Res, 96*(4), 442-450.

SUPPLEMENTAL FIGURES

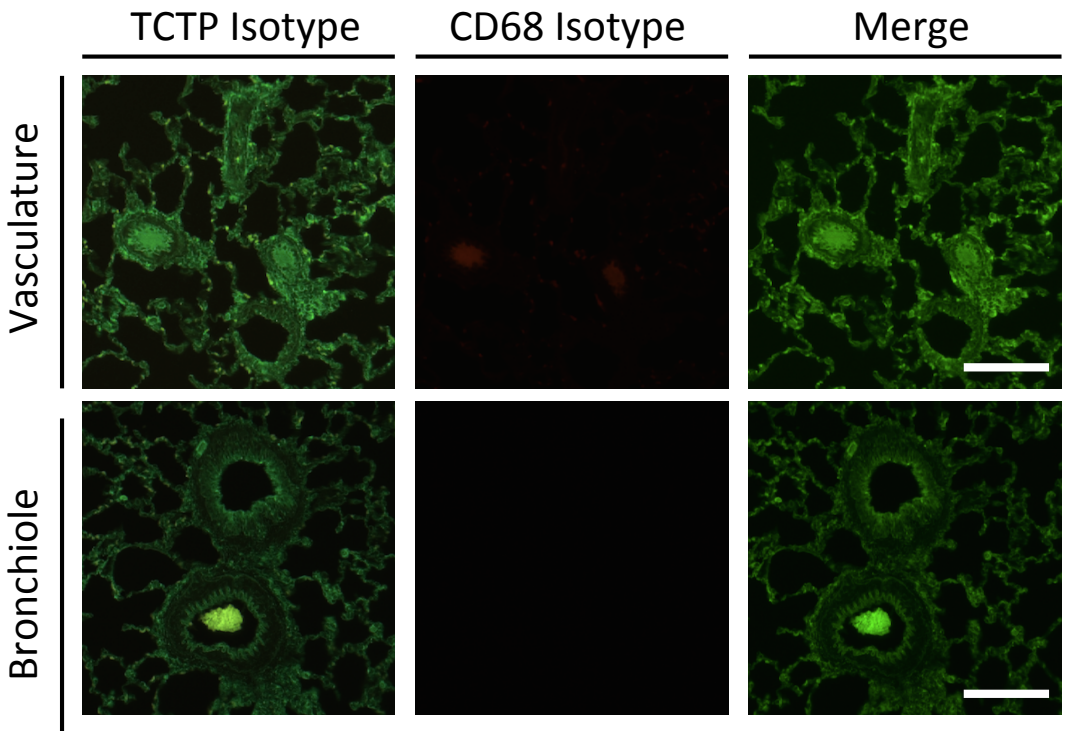

Supplemental Figure 1. Isotype control co-staining for TCTP and CD68 – SU/CH rat lung section. Scale bar = 100μm.

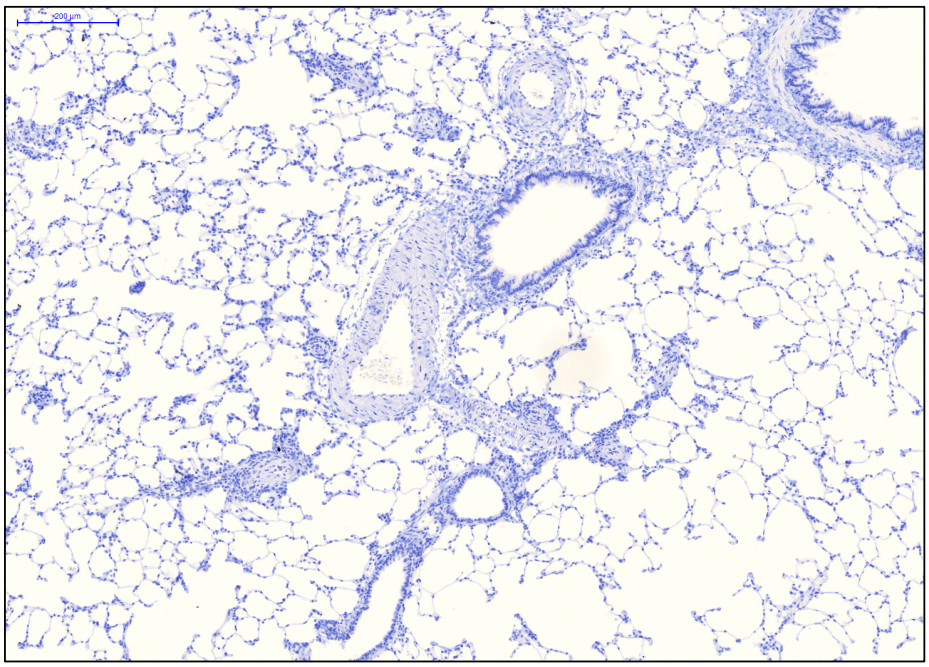

Supplemental Figure 2. Negative control for TCTP immunohistochemistry - SU/CH rat lung section. Scale bar = 100µm.